Progress in Oceanography 92–95 (2012) 50–65

Contents lists available at ScienceDirect

Progress in Oceanography

journal homepage: www.elsevier.com/locate/pocean

Siliceous microorganisms in the upwelling center off Concepción, Chile (36°S): Preservation in surface sediments and downcore fluctuations during the past ~150 years

Gloria E. Sánchez [a], Carina B. Lange [a,b,*], Humberto E. González [a,c], Gabriel Vargas [d], Praxedes Muñoz [e], Carolina Cisternas [f], Silvio Pantoja [a,b]

[a] Centro de Investigación Oceanográfica en el Pacífico Sur-Oriental (COPAS), Universidad de Concepción, Casilla 160-C, Concepción, Chile
[b] Departamento de Oceanografía, Universidad de Concepción, Casilla 160-C, Concepción, Chile
[c] Instituto de Biología Marina, Universidad Austral, Valdivia, Chile
[d] Departamento de Geología, Universidad de Chile, Casilla 13518, Correo 21, Santiago, Chile
[e] Departamento de Biología Marina, Facultad de Ciencias del Mar, Centro de Estudios Avanzados en Zonas Áridas (CEAZA), Universidad Católica del Norte, Larrondo 1281, Coquimbo, Chile
[f] Graduate Program School of Marine and Atmospheric Sciences, Stony Brook University, New York, NY 11794, USA

ARTICLE INFO

Article history:
Available online 18 July 2011

ABSTRACT

We analyzed the temporal patterns of siliceous microorganisms in the water column and their representation in the underlying surface sediments between September 2002 and November 2005, at a fixed station on the shelf off Concepción, Chile (Station 18, 36° 30.80′S and 73° 07.75′W), connecting our results to instrumental records of temperature, salinity, coastal upwelling and freshwater input. The goals of the study were to understand the seasonal representation of siliceous microorganisms in surface sediments and to evaluate the use of this information in the interpretation of past climatic/oceanographic conditions in the area. The implications of seasonal and preservational biases are discussed. Additionally, a 30-cm core collected at the same site and spanning the last ~150 years of sedimentation was also studied in order to provide a record of historical siliceous productivity changes.

Firstly, the analyses focused on diatoms since they were numerically the most prominent microorganisms in the water column and the surface sediments, independent of season and year. In both settings, maxima of the key diatom genera *Chaetoceros* and *Skeletonema* coincided with the spring–summer upwelling period. For the autumn–winter non-upwelling period, significant plankton–sediment discrepancies were observed, with enrichment of moderately robust taxa in the sediments, as well as freshwater diatoms and phytoliths tracing the increased river discharges in winter. Secondly, the downcore analysis revealed a marked decrease in total diatom accumulation rates since the late 19th and throughout the 20th century, which was accompanied by increasing concentrations of lithogenic particles and freshwater diatoms. An alkenone-based sea surface temperature reconstruction in the same core (past ~150 years) and instrumental data show that these changes occurred simultaneously with a general trend of increasing temperatures in the upwelling area off Concepción. Taken together, these signals suggest an intensified influence of ENSO-like variability in the ocean-climate system off central-southern Chile.

1. Introduction

The Humboldt Current System (HCS) is a major Eastern Boundary Upwelling Ecosystem characterized by recurrent coastal upwelling promoting exceptionally high primary productivity, which, in turn, supports a strong fishery (Daneri et al., 2000; Chavez et al., 2008). Off central-southern Chile (Fig. 1A), upwelling activity is markedly seasonal, with the strongest upwelling events during the austral spring–summer (September–March) and downwelling in winter due to the prevalence of strong northerly winds (Fig. 1B). Upwelled waters usually originate from the Equatorial Subsurface Water (ESSW) mass that is transported southward by the Peru–Chile Undercurrent and is characterized by high salinities ($\geqslant$34.5), temperatures <11.5 °C and low dissolved oxygen concentrations (<1 mL L^{-1}) (e.g. Sobarzo et al., 2007a). Upwelling includes a shallowing of the oxygen minimum zone (OMZ), a feature linked to ESSW (Strub et al., 1998). Formations of eddies and filaments are

* Corresponding author at: Centro de Investigación Oceanográfica en el Pacífico Sur-Oriental (COPAS), Universidad de Concepción, Casilla 160-C, Concepción, Chile. Tel.: +56 41 220 4520; fax: +56 41 220 7254.
E-mail address: clange@udec.cl (C.B. Lange).

0079-6611/$ - see front matter © 2011 Elsevier Ltd. All rights reserved.
doi:10.1016/j.pocean.2011.07.014

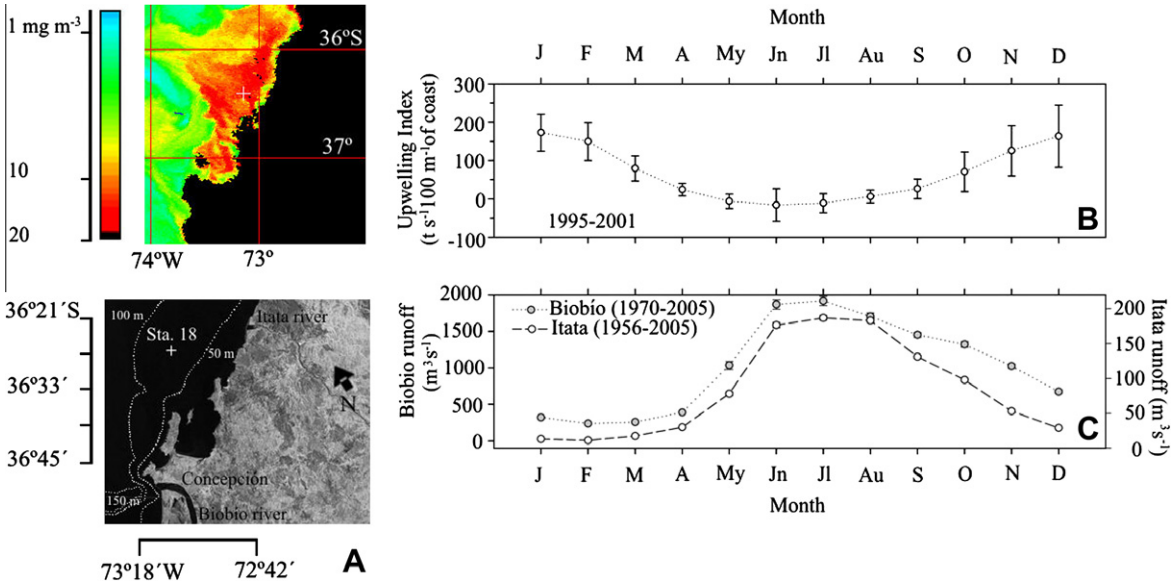

Fig. 1. (A) Study area showing the location of the sampling site (Station 18, cross) on a SeaWiFs chlorophyll *a* color image for the austral spring, 23 October 1998 (upper panel), and on a depth-contour map including the Biobío and Itata rivers (map modified from Google Earth). The color bar indicates chlorophyll *a* concentrations in mg m^{-3}. (B) Monthly mean upwelling index (metric-tons s^{-1} km^{-1}) at 36°S, 74°W taken from www.pfeg.noaa.gov (Transport Indices computed from monthly mean fields from FNMOC six-hourly Atmospheric Pressure at Mean Sea Level analysis fields, 73 × 144). (C) Monthly mean discharges (m^3 s^{-1}) for the Biobío (1970–2005) and Itata (1956–2005) rivers; data from the Dirección General de Aguas de Chile (www.dga.cl). Vertical bars show 1 standard deviation.

common and provide a means for transporting coastal water (and nutrients) offshore (Grob et al., 2003; Hormazábal et al., 2004; Letelier et al., 2004; Morales et al., 2007).

The oceanography off central-southern Chile has been studied in detail by various authors (e.g. Ahumada and Chuecas, 1979; Sobarzo et al., 1997; Letelier et al., 2004), and recently, a special volume on the structure and functioning of this coastal upwelling system was published (Escribano and Schneider, 2007). In brief, the area off Concepción (36°S, Fig. 1A) is considered to be one of the most productive sectors of the Chilean coast, where maximum values of integrated gross primary production of 19.9 g C m^{-2} d^{-1} (November 1998) and 25.8 g C m^{-2} d^{-1} (December 2003) have been reported by Daneri et al. (2000) and Montero et al. (2007), respectively. Phytoplankton biomass also has a strong seasonal signal, with maximal chlorophyll-*a* peaks in the upper 20 m of the water column in December/January every year (Escribano et al., 2007). In addition to the marked seasonality of the upwelling regime, the area off Concepción is also affected by the stratification of the water column, the mixed layer's heat balance (solar radiation in the summer), and the freshwater balance (river outflow and precipitation in winter; Sobarzo et al., 2007a; Thiel et al., 2007). This coastal area receives contributions from two major rivers, the Itata and the Biobío, with average water outflows of 60 ± 65 m^3 s^{-1} (1956–2002) and 993 ± 772 m^3 s^{-1} (1970–2002), respectively (Fig. 1C) (Dirección General de Aguas de Chile, www.dga.cl). The seasonal water discharge is regulated by precipitation and ice melt from the Andes, resulting in discharge maxima between May and October (late fall to early spring), and low input from December to April (summer to early fall) (Fig. 1C). The annual cycle of river discharge and precipitation has an impact on the salinity of the upper 20 m of the water column, with a sharp decrease in salinity in winter; runoff due to snow melt is less important (Sobarzo et al., 2007a). The Biobío and Itata rivers also supply the study area with nutrients associated with the weathering of the Andes and the Coastal Mountain Range (Pineda, 1999).

Elevated spring–summer phytoplankton biomass and primary production promotes high fluxes of organic particles to the seafloor (González et al., 2007) that could cause anoxic conditions in the sediments and the bottom water (e.g. Gutiérrez et al., 2000). Increased vertical fluxes of particulate organic carbon, diatoms and biogenic silica coincide with periods of highest production in the upper water column (González et al., 2007; Sánchez et al., 2008). Furthermore, surface sediments are rich in total organic carbon content (~3–6%; Muñoz et al., 2007) and diatoms (mainly *Chaetoceros* spores and *Skeletonema*; Sánchez et al., 2009). At the sediment–water interface, a flocculent layer composed mainly of phytodetritus can form (e.g., Graco et al., 2001).

The strong seasonality in water column processes, fluxes to the seafloor, and the influence of the OMZ on the continental shelf sediments may vary strongly on interannual to multi-decadal scales given that the region is affected by large-scale phenomena such as the El Niño Southern Oscillation (ENSO), the Pacific Decadal Oscillation and ongoing global climate change.

Transformations associated with the settling of biogenic material from the uppermost layers of the ocean to the seafloor provide clues for understanding the mechanisms involved in the formation of sediments, the supply of food to the deep-sea benthos, and the formation and fate of new and recycled organic matter (Berger et al., 1989). In this work, we analyzed the abundance and composition of siliceous microorganisms (mainly diatoms) in samples from the water column and underlying sediments (surface sediments and downcore) collected at Station 18 located within the upwelling center off Concepción (~36°S), with the following goals: (1) to assess how closely the phytoplankton annual cycle coincides with the pattern reflected in the sedimentary record, linking our results to instrumental records of coastal upwelling and freshwater input; and (2) to deliver a record of siliceous productivity changes for the last ~150 years of sedimentation.

2. Materials and methods

The study site is located ~33 km from the coast on the continental shelf off Concepción (Station 18; 36° 30.80′S; 73° 07.75′W; ~90 m water depth; Fig. 1). Station 18 is one of the fixed time-series stations routinely sampled by the Center for Oceanographic

Research in the eastern South Pacific (COPAS Center) since 2002. We analyzed water column samples and sediments collected between September 2002 and November 2005. Field work was carried out onboard the R/V Kay Kay of the Universidad de Concepción.

2.1. Water column sampling and analysis

Micro-phytoplankton data used in this study were taken, in part, from González et al. (2007), who covered the period September 2002 to May 2005. We added new data, extending the timeframe to November 2005. Samples from St. 18 were collected using 30-L Niskin bottles. These samples were concentrated (10–30 L) by passing them through a 20-μm sieve (final volume of 100 mL), preserved in buffered formalin (4%), and later analyzed for general taxonomic composition and abundance using an inverted microscope Olympus CK2 at 400× (Utermöhl, 1958); see González et al. (2007) for details on methodology. For each monthly sampling, diatom abundance data (cells L^{-1}) were integrated over a water column depth of 40 m, and data are expressed in diatom cells m^{-2}.

2.2. Sediment sampling and analyses

Sediment cores were collected with a mini-multicorer (inner diameter 9.5 mm) (Barnett et al., 1984) on a monthly basis and were sliced continuously into 0.5–1-cm sections using a Plexiglas spatula. Only undisturbed cores with clear overlying water were used. Temporal variability analyses were done on each monthly surface sediment sample (considering the upper 0.5 cm to be "surface sediment") from September 2002 through to November 2005, and on one core (MUC1803) collected in January 2003 for downcore fluctuations (see below). All samples analyzed downcore for the various proxies came from the same core.

Each sediment sample (0–0.5 cm, and downcore) was analyzed for:

(a) Biogenic opal ($\%Si_{OPAL}$). This was determined following the method described by Mortlock and Froelich (1989), which consists in a single extraction of silica with an alkaline solution at 85 °C for 6 h, and measuring the dissolved silicon concentration in the extract by molybdate-blue spectrophotometry at 812 nm. The $\%Si_{OPAL}$ data were converted to concentrations in each sample and are reported in mg g^{-1} dry sediment.

(b) Siliceous microorganisms. For this analysis, wet sediment samples were freeze-dried and ~0.5 g of dry sediment was treated according to the technique described by Schrader and Gersonde (1978). Permanent slides of acid-cleaned material were prepared by placing a defined sample volume (0.2 mL) onto a microscope slide, air-drying, and mounting with Naphrax mounting medium. Qualitative and quantitative analyses of siliceous microorganisms were performed at magnifications of 400× and 1000× using a Zeiss-Axioscope 2 plus microscope with phase-contrast illumination. For diatoms, several traverses across each cover slip were examined depending on microorganism abundances. At least two cover slips per sample were examined in this way. About 300 valves were counted for each cover slip. The counting procedure and definition of counting units for diatoms followed those of Schrader and Gersonde (1978). For silicoflagellates, phytoliths (discrete, solid bodies of opaline silica in epidermal cells of grasses; Alexander et al., 1997; Runge, 1999), chrysophycean cysts (siliceous resting stages of chrysophycean algae that are commonly found in lakes; Smol, 1988), and sponge spicules, a fraction of the slide (1/2 or 1/5 of each cover slip, depending on abundance) was counted. Abundances of taxa and/or microorganism groups are expressed as concentration per gram of dry sediment. Relative abundances of individual diatom species were calculated as a percentage of the total assemblage. Diatoms were identified to the lowest taxonomic level possible, based principally on the works of Hustedt (1930), Cupp (1943). Rivera (1968, 1981), Round et al. (1990), Sims (1996), Tomas (1997), and Witkowski et al. (2000). For *Skeletonema*, we followed the taxonomic changes in the recent literature, and according to Kooistra et al. (2008), the taxon from Concepción belongs to the species *Skeletonema japonicum*. Silicoflagellate species were identified using Takahashi and Blackwelder (1992); all other siliceous microorganisms were counted as groups. The most important siliceous groups and diatom species were also photographed under the electron microscope JSM-6700F of the Stazione Zoologica "Anton Dohrn" in Naples, Italy.

(c) Diatoms. The Shannon–Wiener diversity index (Brower et al., 1998) for each sample was calculated as $H' = -\Sigma\ pi\ log\ pi$, where $pi = ni/N$, pi is the proportion of the total number of individuals per species in each sample, based on ni = number of individuals per species, and N = total number of individuals per sample.

In addition to Si_{OPAL} and siliceous microorganisms, downcore analyses also included the following parameters: (i) bulk sediment density, (ii) magnetic susceptibility, (iii) grain-size, (iv) organic matter content, (v) alkenones and (vi) ^{210}Pb activities.

Dry bulk density (DBD) was calculated from the mass percentage of water and density of solids, where ρ_{solid} is 2.65 g cm^{-3} and $\rho_{H2O\ interstitial}$ is 1.025 g cm^{-3} (Bloesch and Evans, 1982).

Magnetic susceptibility (Ellwood, 1980) was measured on wet sediment samples using the Spinning Specimen Magnetic Susceptibility Anisotropy Meter KLY model developed by 3S AGIC Inc. The average value of each sample (section) was divided by its weight, yielding a normalized value for each 1-cm core section (magnetic susceptibility per unit weight, SI).

Grain size laser analysis was performed on the total sediment using Hydro-G Mastersizer 2000 equipment and applying standard analytical procedures recommended for specific materials. Mean grain size parameters are accompanied by the corresponding standard deviation values calculated from the total grain size distribution.

Organic matter content was estimated as percentage weight loss after ignition at 550 °C in a muffle furnace (% LOI).

Alkenones $C_{37:2}$ and $C_{37:3}$ were determined according to the methodology described by Prahl and Wakeham (1987) and Prahl et al. (1988). About 3 g of wet sediment were extracted with dichloromethane–methanol. Prior to extraction, a recovery standard (*n*-heptacosanone) was added to the sediment. The lipid fraction was subjected to column chromatography to separate lipid functional groups from the total extract. The fractions containing C_{37} alkenones were concentrated and dissolved in iso-octane and 5α-cholestane, and then an internal standard (C_{27} alkenones) was added; the fractions were analyzed in a Shimadzu Gas Chromatograph equipped with a capillary column (Rtx-5 m, 0.22 μm, 0.32 mm i.d. ×30 m, J&W Scientific) and a flame ionization detector. The separation of compounds was carried out with hydrogen as a carrier gas at 6.37 mL/min (~10 psi column head pressure). The temperature program was as follows: initial column temperature at 50 °C for 1 min, increased to 120 °C at 30 °C/min, increased to 300 °C at 6 °C/min, isothermal at 300 °C/48 min; total run time: 61.3 min. Peaks were identified by their retention times. Data are expressed in μg g^{-1}.

Sea surface temperature (SST) was calculated using the linear calibration function relating the unsaturation index $U^{K'}_{37}$ to growth

temperature T; $U^{K'}_{37} = 0.033T + 0.043$ (Prahl and Wakeham, 1987). An alkenone-derived SST reconstruction from St. 18 was compared to the record from the nearby St. 26 (located 26 nautical miles from the coast, at 123 m water depth) published by Vargas et al. (2007).

Accumulation rates of Si_{OPAL} and the various siliceous microorganisms were calculated based on their respective concentrations within each 0.5 or 1-cm intervals of the core, multiplied by the dry bulk density at each core depth and the average sedimentation rate estimated from ^{210}Pb activities. Data are expressed in mg cm^{-2} yr^{-1} and in organisms cm^{-2} yr^{-1}, respectively.

^{210}Pb activities were assessed mainly by alpha spectrometry of its daughter, ^{210}Po, using ^{209}Po as a yield tracer (Flynn, 1968). The ^{210}Po activity was counted by a CANBERRA QUAD alpha spectrometer, model 7404, requiring 24 to 48 h to achieve the desired counting statistics (4–10% 1σ errors). The activity of ^{210}Po, assumed to be in secular equilibrium with ^{210}Pb, was calculated using the ratio between the natural radionuclide and the tracer, which is multiplied by the activity of the tracer at the time of plating. All data were corrected to the time of plating, considering the decay of ^{210}Po (half life: 138 days) that occurred between plating and counting. Because of the short period elapsed between the collection date and the time of the sample analyses (<6 months) compared to the half life of ^{210}Pb (22.3 years), the calculated activities were not corrected for this delay (see Muñoz et al., 2004, for details on methodology). The excess ^{210}Pb was calculated by subtracting the background determined by asymptotic activity at depth (1.5 ± 0.1 dpm g^{-1}) assumed to be in equilibrium with ^{226}Ra within the sediment (McCaffrey and Thomson, 1980; Cochran et al., 1998). This value was similar to ^{226}Ra measured in the area (1.1 ± 0.2 dpm g^{-1}; Muñoz et al., 2004). The standard deviations of ^{210}Pb inventories were calculated by propagating the counting uncertainties of ^{210}Pb and the standard error introduced by the background estimation (Bevington and Robinson, 1992).

2.3. Instrumental records

The monthly mean upwelling index (tonnes/s/km) in Fig. 1B was taken from http://www.pfeg.noaa.gov, which includes transport indices computed from monthly mean fields from FNMOC six-hourly Atmospheric Pressure at Mean Sea Level analysis fields (73 × 144) at 36°S and 74°W. The daily upwelling index shown in Fig. 2A was calculated from wind speed and direction according to the water mass transport equation by Bakun (1975). Wind data were obtained from the Carriel Sur meteorological station (36° 46′S; 73° 04′W). See, Cornejo et al. (2007) and González et al. (2007), for details.

Data on river discharges and suspended sediments for the Biobío and Itata rivers (Figs. 2C and 3) were measured at the river mouths and were provided by the Dirección General de Aguas de Chile (www.dga.cl). Precipitation data (Fig. 3) were taken from the Climate Explorer Time-Series web site (http://climexp.knmi.nl/getprcpall.cgi?someone@somewhere+85682+CONCEPCION).

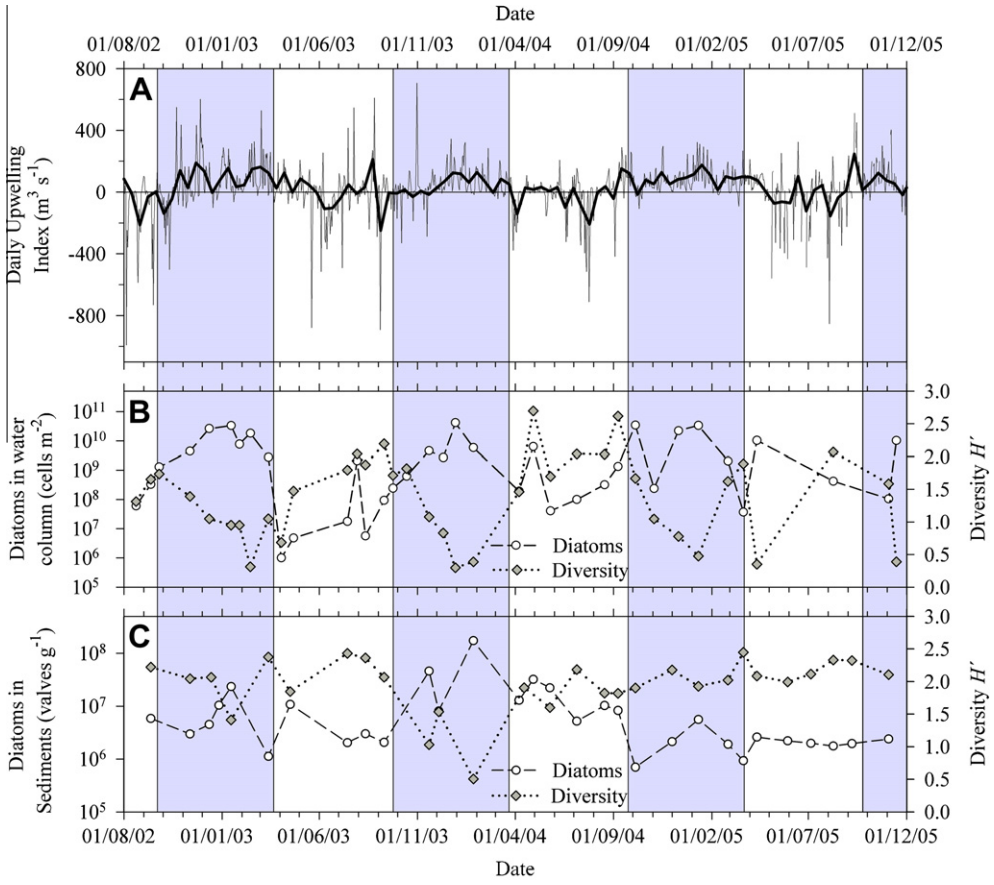

Fig. 2. Upwelling and diatoms. Comparison between water column and surface sediments at COPAS Time-Series Station 18, from September 2002 through November 2005. (A) Daily upwelling index (m^3 s^{-1}), according to the water mass transport equation of Bakun (1975). Wind data were obtained from the Carriel Sur meteorological station (36° 46′S; 73° 04′W). The thick line represents 7-days running mean. (B) Total diatom abundance (cells m^{-2}) and diversity (Shannon–Wiener diversity index, H') in the water column: monthly diatom abundance data integrated over a water column depth of 40 m; data are expressed in diatom cells m^{-2}. (C) Total diatom abundance and diversity (H') in the surface sediments (0–0.5 cm). Abundance is expressed as diatom valves g^{-1} dry sediment. Dates above and below the figure are given in dd/mm/yy.

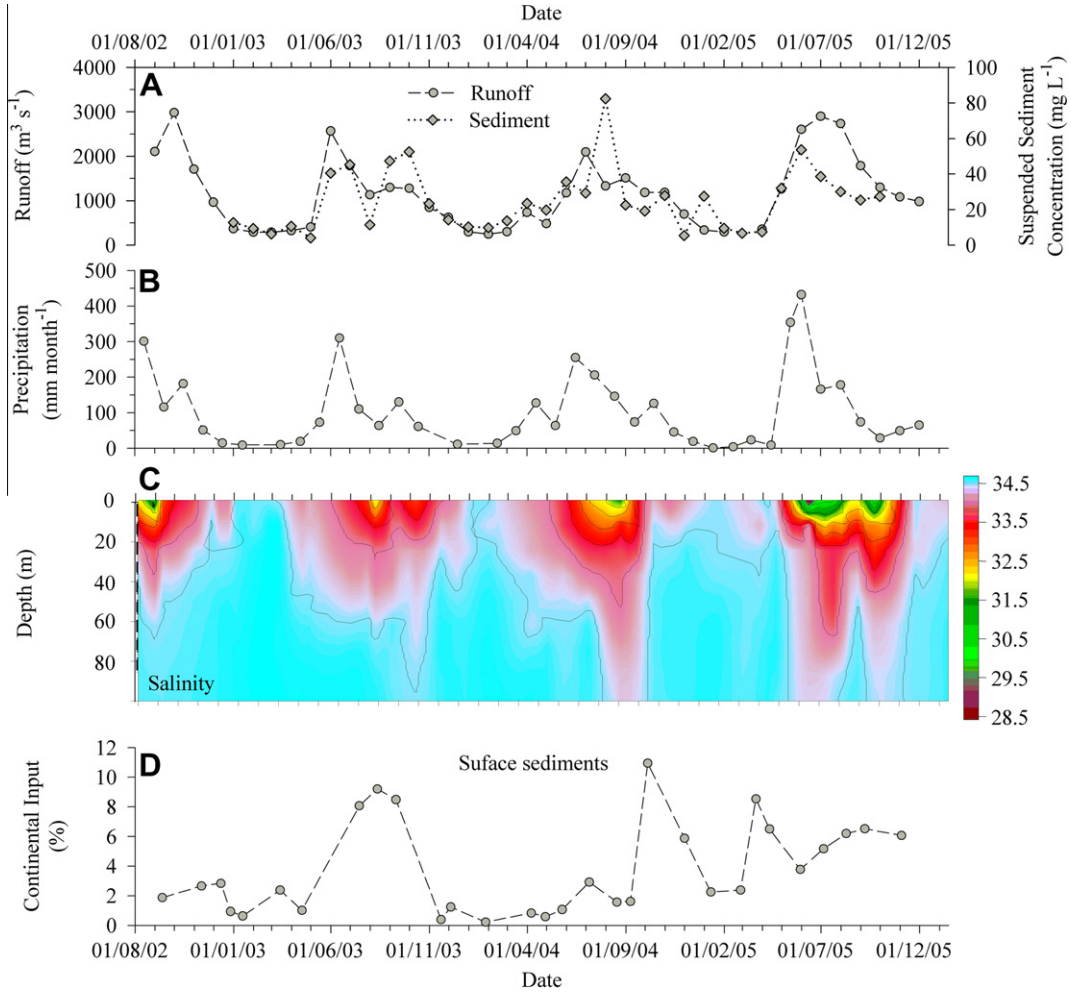

Fig. 3. The signal of continental influence in the water column and in the surface sediments, COPAS Time-Series Station 18 (September 2002–November 2005). (A) Biobío river discharge and suspended sediment measured at the river mouth (monthly averages in m^{-3} s^{-1} and mg L^{-1}, respectively). (B) Average monthly precipitation measured at Concepción Carriel Sur Airport (mm $month^{-1}$). (C) Sea salinity at St. 18 from COPAS Time-Series Study (Escribano et al., 2007). (D) The combined contribution of freshwater diatoms, chrysophycean cysts and phytoliths (continental input %) in the surface sediments of St. 18. River data from the Dirección General de Aguas de Chile (www.dga.cl), and precipitation data from the Climate Explorer Time-Series. Dates above and below the figure are given in dd/mm/yy.

3. Results

3.1. Plankton vs. surface sediments at Station 18

The spring and summer upwelling index from 2002 to 2005 was positive most of the time whereas, in late autumn and winter, it was generally negative (Fig. 2A). Monthly diatom abundance data integrated over a water column depth of 40 m fluctuated between $\sim 1 \times 10^6$ cells m^{-2} (3 April 2003) and 4.1×10^{10} cells m^{-2} (30 December 2003); abundances $>10^9$ cells m^{-2} always coincided with the upwelling period (Fig. 2B). In general, the specific diversity of diatoms, H', was inversely related to their abundance. The highest abundances in spring–summer usually yielded the lowest diversities (Fig. 2B).

A total of 87 diatom taxa were identified over the 2002–2005 sampling period. Because this number included cases in which organisms were identified only to the genus level, it may underestimate the actual number of species present in the area. Only a handful of species/species groups dominated the assemblage in the water column (Table 1). In terms of their relative abundances over an annual cycle, the main components of the diatom assemblage were *S. japonicum* (annual average ~54%) and several species of the genera *Chaetoceros* (~30%) and *Thalassiosira* (~8%) (Table 1). A clear seasonal pattern could also be discerned. For example, *Skeletonema* and *Chaetoceros* dominated in spring–summer (contributing >80% to the total assemblage); *Thalassiosira* spp. in autumn (and secondarily in winter); *Pseudo-nitzschia* spp., *Asterionella japonica*, *Thalassionema nitzschioides*, and *Cylindrotheca closterium* were most abundant in winter; and *Detonula pumila* predominated in autumn–winter (Table 1).

By examining the seasonal fluctuations of diatoms in the plankton, we attempted to understand the importance of seasonal events (and the associated fluxes to the seafloor) and their imprint in the sedimentary record. In the surface sediments (upper 0.5 cm of the sediment column) of St. 18, diatoms were numerically the most prominent group independent of season and year; they accounted for >85% of the total siliceous microorganism assemblage. Their overall abundance from 2002 to 2005 fluctuated between 7×10^5 valves g^{-1} (5 October 2004) and 1.7×10^8 valves g^{-1} (27 January 2004; Fig. 2C); maxima coincided with the spring–summer period (Fig. 2C). Although it was evident that the direction of change was similar in both the water column and the sediments, the magnitude of the temporal variations was less in the sediments compared with the water column: ~2 vs. ~4 orders of magnitude, respectively (Fig. 2B and C).

The specific diversity of diatoms (H') varied between 0.5 and 2.5 with an overall pattern similar to the one in the water column from September 2002 through to September 2004. Thereafter, diversities

Table 1
Comparison between the relative contribution of the most abundant diatoms in the water column and the surface sediments. Values are mean percentages for each season and annually (from September 2002 to November 2005). A: autumn, W: winter, Sp: spring, Su: summer; dashed lines = no occurrence.

Diatoms	Water column					Surface sediments				
	A	W	Sp	Su	Annual	A	W	Sp	Su	Annual
Skeletonema japonicum	10.47	11.18	48.75	60.93	53.60	11.92	2.73	1.89	42.97	30.95
Chaetoceros spp. (*Ch. compresus*, *Ch. sociales*, *Ch. radicans*) veg. cells	8.11	12.02	30.74	32.39	30.06	0.70	–	0.74	0.01	0.21
Thalassiosira spp. (*T. minuscula*, *T. aestivalis*)	56.07*	13.68	7.01	2.62	7.58	1.37	1.65	2.12	0.67	1.01
Pseudo-nitzschia spp.	3.93	19.24	4.81	2.01	3.10	0.01	0.04	–	0.01	0.01
Chaetoceros spp. (*Ch. didymus*, *Ch. curvisetus*, *Ch. socialis*) resting spores	2.18	0.25	2.74	0.08	0.96	81.94	83.36	89.44	55.18	65.70
Freshwater diatoms	0.54	0.25	1.92	0.81	1.10	0.88	3.68	1.68	0.28	0.71
Rhizosolenia, *Guinardia*, *Proboscia* and *Dactyliosolen*	0.66	1.88	0.30	0.03	0.17	0.01	0.08	0.03	0.01	0.01
Odontella spp. (*O. aurita*, *O. longicruris*)	0.05	0.05	0.11	0.06	0.07	0.75	1.33	0.78	0.25	0.45
Thalassionema nitzschiodes	–	2.47	0.18	<0.01	0.08	0.24	1.20	0.22	0.11	0.20
Actinoptychus spp. (*A. senarius*, *A. vulgaris*)	<0.01	<0.01	<0.01	0.02	0.01	0.83	2.78	1.32	0.22	0.57
Detonula pumila	8.18	13.23	0.93	0.07	1.00	–	–	–	–	–
Cerataulina sp.	0.39	0.08	0.26	0.02	0.11	–	–	–	–	–
Asterionella japonica	<0.01	12.56	0.60	0.16	0.41	–	–	–	–	–
Eucampia spp. (*E. cornuta*, *E. zodiacus*)	0.64	0.05	0.07	0.02	0.08	–	–	–	–	–
Leptocylindrus spp. (*L. danicus, L. minimus*)	0.90	0.32	0.87	0.06	0.35	–	–	–	–	–
Cylindrotheca closterium	0.02	2.17	0.02	0.02	0.05	–	–	–	–	–

* The high mean percentage is due to sporadic blooms of *Thalassiosira* in early autumn.

differed markedly, with very low values in the water column for January (due to a maximum in *Skeletonema*), April (due to a *Thalassiosira minuscula* bloom), and November 2005 (*Chaetoceros* maximum). Diversity in the sediments, on the other hand, remained rather constant throughout 2005 (Fig. 2B and C).

The surface sediments had two major diatom components: (1) the resting spores of the genus *Chaetoceros* (which were invariably the ones that dominated the sedimentary imprint), with an overall annual contribution of ~66% to the total diatom assemblage and the highest relative abundances (>80%) in autumn, winter, and especially in spring (Table 1); and (2) *S. japonicum*, the second most important diatom in the sediments, contributing 43% to the preserved summer assemblage and ~31% annually (Table 1). The water column-sediment pattern of the genus *Chaetoceros* included high abundances of vegetative cells and minor abundances of spores in the water column, whereas the reverse was true for the surface sediments. In general, about ten species/species groups found in the water column also occurred in surface sediments, but their relative abundances differed from their mean percent values in the plankton and six were missing in the sediment (Table 1).

The mean relative abundance of freshwater diatoms in the surface sediments varied from <1% in summer-autumn to almost 4% in winter (Table 1). The most important species in this group were *Epitemia zebra*, *Cymbella affinis*, *Cymbella ventricosa* var. *ventricosa*, *Fragilaria construens*, *F. vaucheriae* var. *vaucheriae*, *Rhoicosphenia curvata*, *Diploneis subovalis*, and *Aulacoseira granulata*. In Fig. 3, we illustrate the monthly fluctuations of river discharges and suspended sediments, precipitation in Concepción, salinity in the water column at St. 18, and the relative abundance of freshwater diatoms, phytoliths and chrysophycean cysts combined in the surface sediments of St. 18 as a proxy for continental input. The water column pattern of continental influence (Fig. 3A–C), which was strongest from late fall until well into the spring (see Introduction), left its imprint in the surface sediments, as recorded by these siliceous microorganisms of continental origin. The highest values ($\geqslant$8%) were observed in July–September 2003 (winter), October 2004 (early spring), and March 2005 (early autumn), and sustained values of >5% were seen from July to November 2005 (Fig. 3D).

3.2. Downcore fluctuations

3.2.1. General sediment characteristics of core MUC1803 and siliceous micoorganisms

Sediments at St. 18 were homogeneous, fine-grained, olive to olive-gray hemipelagic mud (Munsell Soil Color Chart # 7.5Y). Sediment dry bulk density increased downcore from 0.1 g cm^{-3} at the surface to ~0.6 g cm^{-3} at the base (30 cm depth in core); the largest increments were observed at 0–3 cm and at 12–15 cm depth in core (Fig. 4A). Magnetic susceptibility exhibited lower values at the bottom of the core, below 27 cm; values increased rapidly between 27 and 23 cm, and were rather constant in the upper 23 cm (Fig. 4B). Mean grain size values ranged between 20 and 40 μm, with lower values at 6–10 cm and below 26 cm depth in core (Fig. 4C).

The sediments had high organic matter content, which varied between 21% at the top and ~15% at the base of the core (Fig. 4D). Biogenic opal content (Si_{OPAL}) averaged 107 ± 8.9 mg g^{-1} dry sediment and showed a clear increasing trend downcore (Fig. 4E). The concentration of alkenones was low and varied greatly (0.08–1.88 μg g^{-1} dry sediment), especially in the upper 18 cm of the core (Fig. 4F).

Skeletal remains of siliceous microorganisms were abundant in core MUC1803. Diatom valves and resting spores, sponge spicules, chrysophyceae cysts, and phytoliths were commonly observed in the 30-cm-long core; silicoflagellates and radiolarians only occurred sporadically (Fig. 5). The concentration of the total siliceous microorganism assemblage (organisms per g of dry sediment) ranged from 1.65 × 10^6 to 4.30 × 10^7 organisms g^{-1}. It was dominated by diatoms, which contributed >95% of the total siliceous assemblage.

All sediment samples showed good preservation of diatom valves (Fig. 5), allowing the identification of 157 diatom taxa (Table 2). Diatom diversity (H') ranged from 1.4 (at 19–20 cm) to 2.4 (at 4–5 cm); in general, lower values corresponded to abundance maxima when assemblages were dominated by *Chaetoceros* spores. Few diatoms were abundant; 13 species or species groups accounted for >90% of the whole diatom assemblage (Table 3). The main contributors were *Chaetoceros* spores (*C. radicans*/*cinctus* 38%, *C. constrictus*/*vanheurckii* 17%, *C. debilis* 10%, *C. diadema* 6%, and *C. coronatus* 3.5%; Fig. 5A–D). The spore assemblage was accompanied by *S. japonicum* (~10%), *Thalassiosira eccentrica* (3.5%), several freshwater diatoms (~2%), *Actinopthychus senarius*, and *T. nitzschioides*, among others (Fig. 5E–L).

3.2.2. Age model

The age model of multicore MUC1803 was based on ^{210}Pb measurements. At St. 18, the $^{210}Pb_{xs}$ (in excess) showed exponential decay below a mixed layer of 3–4 cm (Fig. 6A) down to 19 cm core depth, where it abruptly decreased to background levels. The age in each section was determined from the ^{210}Pb inventories in excess, as follows: $t_z = -\tau_{210} \ln(I_z/I_0)$, where τ_{210} is the radioactive

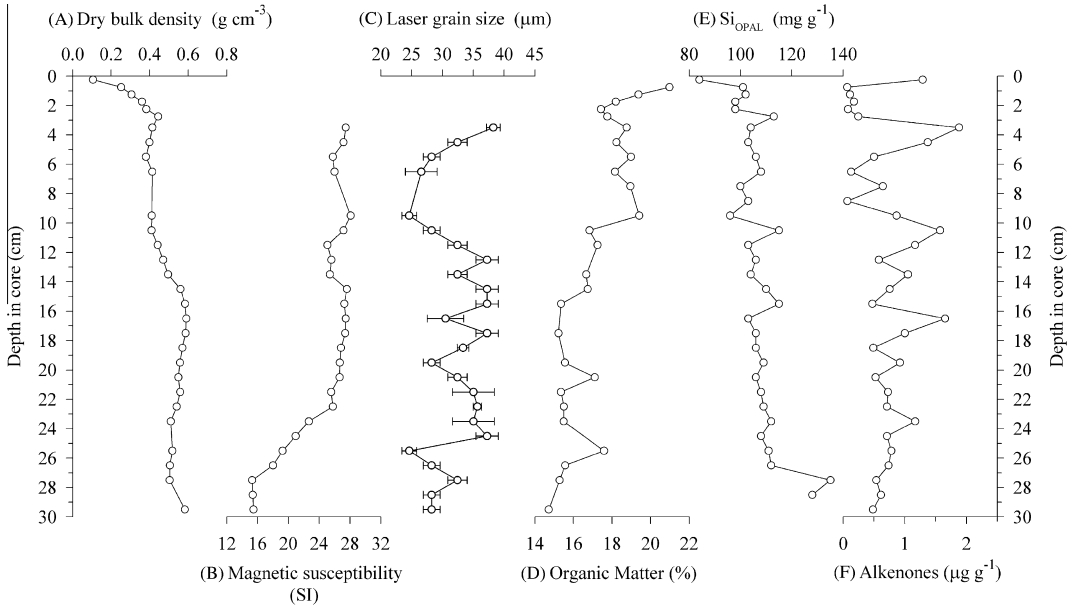

Fig. 4. Downcore profiles for core MUC1803 collected at Station 18 off Concepción. (A) Dry bulk (g cm^{-3}). (B) Magnetic susceptibility. (C) Mean grain size and standard deviation (μm). (D) Total organic matter (TOM %). (E and F) Concentrations of biogenic opal (Si_{OPAL} mg g^{-1} dry sediment) and alkenones (μm g^{-1} dry sediment).

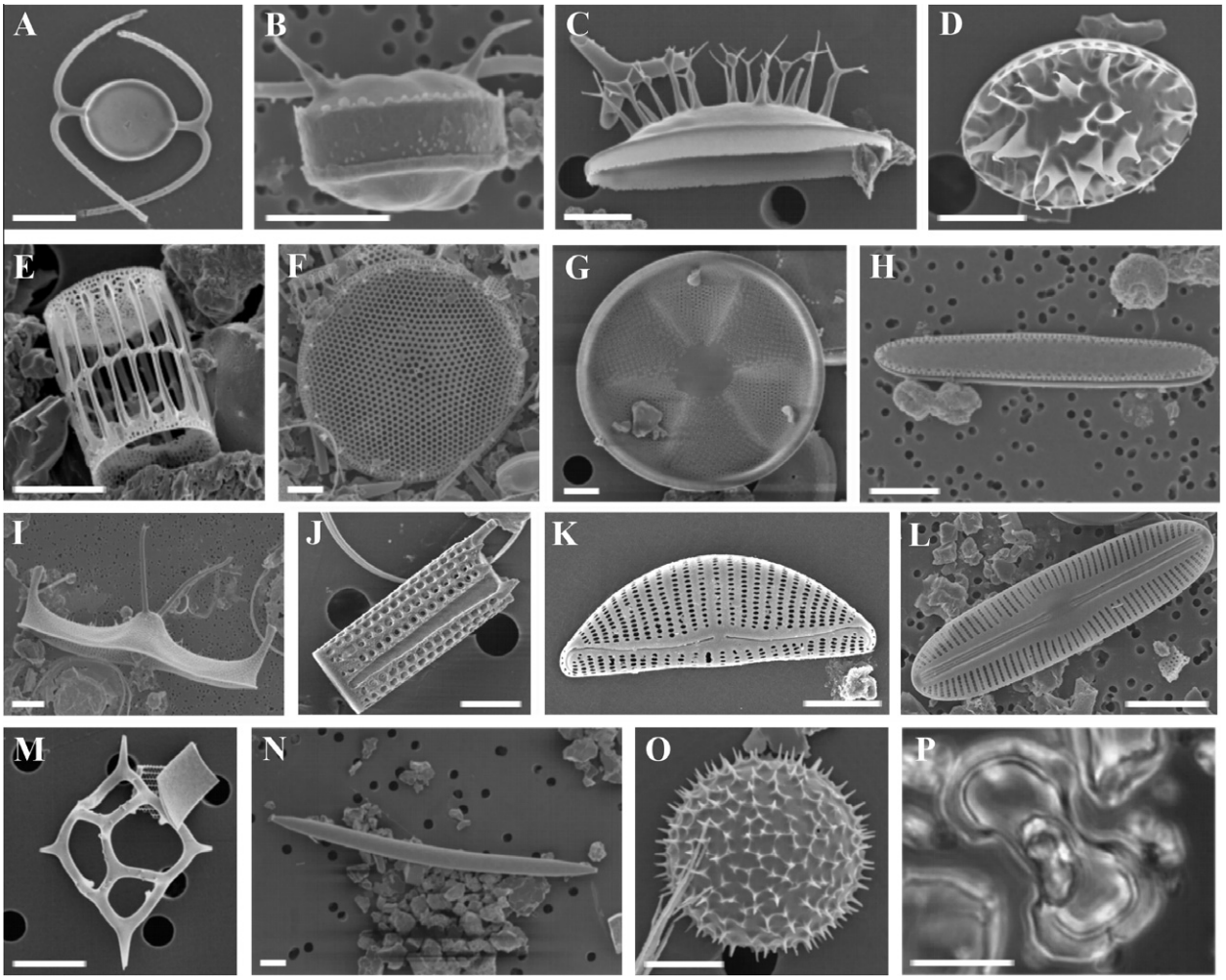

Fig. 5. Siliceous microorganisms preserved in the sedimentary column of core MUC1803 collected at St. 18 off Concepción. (A–O) Scanning Electron Microscopy. (P) Light Microscopy. (A–D) Spores of the diatom genus *Chaetoceros*: (A) *C. radicans*/*cinctus*. (B) *C. debilis*. (C) *C. diadema*. (D) *C. coronatus*. (E) *Skeletonema japonicum*. (F) *Thalassiosira eccentrica*. (G) *Actinoptychus senarius*. (H) *Thalassionema nitzschioides*. (I) *Odontella longicruris*. (J–L) Freshwater diatoms. (J) *Aulacoseira granulata*. (K) *Cymbella ventricosa* var. *ventricosa*. (L) *Diploneis subovalis*. (M) Silicoflagellate *Dictyocha messanensis*. (N) Sponge spicule. (O) Chrysophycean cyst. (P) Phytolith. Bar = 5 μm for A–L and O; Bar = 20 μm for M, N and P.

Table 2
Diatoms in the sedimentary record (MUC1803) at Station 18, off Concepción, grouped into categories according to habitat and/or distribution (this grouping was based on ecological characteristics and geographical distributions, as stated in well-known bibliographies (Cupp, 1943; Rivera, 1968, 1981; Round et al., 1990; Sims, 1996; Witkowski et al., 2000; Romero and Hebbeln, 2003)).

Upwelling	Coastal planktonic, temperate, and cosmopolitan
Chaetoceros coronatus Gran*	*Actinocyclus curvatulus* Janisch
C. debilis Cleve*	*Bacteriastrum* sp. Shadbolt
C. diadema (Ehrenberg) Gran*	*Coscinodiscus marginatus* Ehrenberg
C. didymus Ehrenberg* and veg. cells	*C. oculus-iridis* Ehrenberg
C. radicans Gran/*C. cinctus* Schütt*	*C. radiatus* Ehrenberg
Skeletomena japonicum Zingone and Sarno	*Cyclotella litoralis* Lange and Syvertsen
Thalassionema nitzschioides var. *nitzschioides* (Grunow) Mereschkowsky	*Dimeregrama* sp. Ralfs
Chaetoceros spp.*	*Ditylum brightwellii* (West) Grunow in Van Heurck
	Melosira sol (Ehrenberg) Kützing
Non-planktonic (benthic, epiphytic, epipelic)	*Nitzschia bilobata* Smith
Cocconeis californica (Grunow) Grunow var. *antarctica*	*Proboscia alata* (Brightwell) Sundström
C. californica (Grunow) Grunow var. *californica*	*Rhizosolenia imbricata* "group" Brightwell
C. californica (Grunow) Grunow var. *lengana* Rivera	*Stephanopyxis turris* (Greville) Ralfs
C. costata Gregory var. *costata*	*Thalassiosira anguste-lineata* (Schmidt) Fryxell and Hasle
C. costata Gregory var. *hexagona* Grunow	*T. eccentrica* (Ehrenberg) Cleve
C. costata Gregory var. *pacifica* (Grunow) Grunow	*T. oestrupii* var. *venrickae* Fryxell and Hasle
C. diminuta Pantocsek var. *diminuta*	*T. pacifica* Gran and Angst
C. dirupta Gregory var. *dirupta*	*T. poro-irregulata* Hasle and Heimdal
C. fasciolata (Ehrenberg) Brown	*T. poroseriata* (Ramsfjell) Hasle
C. pellucida Hantzsch var. *minor* (Ehrenberg) Grunow	
C. *placentula* Ehrenberg var. *euglypta* (Ehrenberg) Grunow	**Tycoplanktonic**
C. placentula Ehrenberg var. *intermedia* (Héribaud and Peragallo) Cleve	*Actinoptychus senarius* (Ehrenberg) Ehrenberg
C. placentula Ehrenberg var. *rouxii* (Héribaud and Brun) Cleve	*A. vulgaris* Schumann
C. scutellum Ehrenberg var. *scutellum*	*Paralia sulcata* (Ehrenberg) Cleve
Diplomenora sp. Blazé	
Diploneis didyma Ehrenberg	**Warm-temperate**
Entopyla australis (Ehrenberg) Ehrenberg	*Azpeitia africana* (Janisch ex Schmidt) Fryxell and Watkins
Grammatophora arcuata Ehrenberg var. *arcuata*	*A. nodulifera* (Schmidt) Fryxell and Sims
G. hamulifera Kützing	*Chaetoceros lorenzianus* Grunow
G. marina (Lyngbye) Kützing	*Coscinodiscus janischii* Schmidt
G. undulata Ehrenberg	*Fragilariopsis doliolus* (Wallich) Medlin and Sims
Nitzschia parvula Smith	*Nitzschia bifurcata* Kaczamarka and Licea
Tabularia sp. Williams and Round	*Odontella longicruris* Hoban
	T. oestrupii var. *oestrupii* Fryxell and Hasle
Taxa identified to genus	*Stephanopyxis palmeriana* (Greville) Grunow
Thalassiosira sp. 1 Cleve	*Thalassionema nitzschioides* var. *parva* (Heiden) Moreno-Ruíz
Thalassiosira sp. 2 Cleve	*Thalassiosira endoseriata* Hasley and Fryxell
Thalassiothrix sp. Cleve and Grunow	*T. lineata* Jousé
	T. mendiolana Hasle et Heimdal
Freshwater	*Navicula capitata* Ehrenberg var. *hungarica* (Grunow) Ross
Achnanthes hauckiana Grunow var. *rostrata* Schulz	*N. decussis* Oestrup
A. lanceolata var. *dubia* Grunow	*N. dicephala* var. *elginensis* (Gregory) Cleve
A. pinnata Hustedt	*N. effrenata* Krasske
Amphipleura lindheimer Grunow var. *neotropica* Freguelli	*N. lapidosa* Krasske
Amphora splendida Rivera	*N. lateropunctata* Wallace
Asterionella formosa Hassall	*N. lyra* Ehrenberg
Aulacoseira granulata (Ehrenberg) Simonsen	*N. mutica* Kützing var. *tropica* Hustedt
Ceratoneis arcus (Herenberg) Kützing v. *arcus*	*N. pseudoreinhardtii* Patrick
C. arcus var. *linearis* Holmboe	*N. pupula rectangularis* (Gregory) Grunow
Cyclotella meneghiniana Kützing	*N. radiosa* Kützing var. *radiosa*
C. stelligera (Cleve and Grunow) Van Heurck	*N. rhynchocephala* Kützing
Cymbella affinis Kützing	*N. salinarum* Grunow var. *intermedia* (Grunow) Cleve
C. cymbiformis Agardh	*N. simula* Patrick
C. sinuata Gregory	*N. viridula* var. *avenacea* (Brébisson ex Grunow) Van Heurck
C. tumida (Brébisson) Van Heurck	*Neidium bifurcatum* Heiden
C. ventricosa Kützing ver. *ventricosa*	*N. iridis* (Ehrenberg) Cleve var. *iridis*
Diatoma hiemale (Lyngbye) Heiberg var. *quadratum* (Kützing) Ross	*Nitzschia acicolariodes* Hustedt var. *acicularioides*
D. tenue Agardh var. *tenue*	*N. amphibia* Grunow
Diploneis subovalis Cleve	*N. kutzingiana* Hilse
Epithemia sorex Kützing var. *sorex*	*N. linearis* (Agardh) Smith var. *linearis*
E. zebra (Ehrenberg) Kützing	*N. thermalis* (Ehrenberg) Auerswald var. *minor* Hilse
Eunotia fallax Cleve var. *gracillima* Krass.	*Opephora martyi* Héribaud
E. flexiosa (Brébisson) var. *linearis* Okuno	*Pinnularia abaujensis* var. *subundulata* (Mayer and Hustedt) Patrick
E. pectinalis var. *undulata* (Ralfs) Rabenhorst	*P. borealis* Ehrenberg
E. pectinalis var. *minor* (Kützing) Rabenhorst	*P. brebissonii* var. *diminuta* (Grunow) Cleve
E. sudetica Müller	*P. brevicosta* var. *sumatrana* Hustedt
Fragilaria capucina Desmazières var. *lanceolata* Grunow	*P. brevicostata* Cleve var. *intermedia* Manguin
F. construens var. *venter* (Ehrenberg) Grunow	*P. nobilis* Ehrenberg var. *nobilis*
F. pinnata var. *minutissima* Grunow	*P. pinedana* Rivera
F. pinnata Ehrenberg var *pinnata*	*P. substomatophora* Hustedt var. *substomatophora*
F. vaucheriae (Kützing) Petersen	*P. termitina* (Ehrenberg) Patrick var. *termitita*
Frustulia vulgaris (Thwaites) De Toni	*P. tropica* Hustedt var. *densestriata* Rivera

(*continued on next page*)

Table 2 (*continued*)

Upwelling	Coastal planktonic, temperate, and cosmopolitan
Gomphonema acuminatum Ehrenberg var. *acuminatum*	*Rhoicosphenia curvata* (Kützing) Grunow ex Rabenhorst
G. constrictum Ehrenberg	*Rhopalodia gibba* var. *ventricosa* (Kützing) Peragallo and Peragallo
G. hebridense Gregory	*R. musculus* (Kützing) Müller
G. montatum Schumann var. *montanum*	*Surirella ovalata* var. *smithii* Cleve-Euler
G. montatum var. subclavatum Grunow	*Stauroneis anceps* Ehrenberg var. *anceps*
G. parvulum var. *micropus* (Kützing) Cleve	*S. phoenicenteron* f. *gracilis* (Ehrenberg) Hustedt
G. pseudoexiguum Simonsen	*Synedra acus* Kützing var. *acus*
Gomphonema sp. 1 Ehrenberg	*S. parasitica* var. *subconstricta* (Grunow) Hustedt
Gomphonema sp. 2 Ehrenberg	*S. radians* Kützing var. *radians*
Gyrosigma spencerii (Quekett) Griffith and Henfrey var. *spenceri*	*S. socia* Wallace var. *socia*
Meridion circulare var. *constricta* (Ralfs) Van Heurck	*S. ulna* (Nitzsch) Ehrenberg
Navicula anglica Ralfs var. *subsalsa* (Grunow) Cleve	

* Resting spores.

Table 3
Main diatoms in the sedimentary record (core MUC1803) at Station 18, off Concepción, expressed as average contribution (%) of species and/or species groups for the entire sediment column. Species with >0.5% overall relative abundance were ranked in decreasing order of importance.

Species	Station 18 Core MUC 1803	
	Rank	Average percent
Chaetoceros radicans/cinctus	1	38.4
Ch. constrictus/vanheurckii	2	16.8
Ch. debilis	3	10.3
Skeletonema japonicum	4	9.6
Ch. diadema	5	6.2
Ch. coronatus	6	3.5
Thalassiosira eccentrica	7	3.5
Freshwater diatoms	8	2.3
Actinoptychus senarius	9	1.8
Thalassionema nitzschiodes var. *nitzschioides*	10	1.6
Odontella longicruris	11	1.3
Actinocyclus curvatulus	12	0.9
Coscinodiscus spp. (*C. radiatus, C. marginatus*)	13	0.5

mean life of ^{210}Pb (32.1 yr) and I_0 and I_z are the excess ^{210}Pb inventories in the core and below depth z, respectively. This method (constant rate of the supply model; CRS) assumes a constant input of ^{210}Pb, which is unaffected by changes in sediment type or sedimentation rate and constant porosity (Appleby and Oldfield, 1978; McCaffrey and Thomson, 1980). The age model is shown in Fig. 6B.

Below the mixed layer, a constant mass accumulation rate of 0.095 ± 0.005 g cm^{-2} yr^{-1} was determined, considering sediment compaction. ^{210}Pb$_{xs}$ allowed estimating ages down to 21 cm core depth, and revealed that the core captured about 150 years of sediment deposition. Considering a constant mass acumulation rate, it was possible to extrapolate an age of ~1840 AD at the base of the core (30 cm; Fig. 6B).

In the interpretation of the ^{210}Pb$_{xs}$ data in the core presented here, no independent radionuclide chronometer was used to validate the sedimentation rate obtained. We assumed that the core top was intact during sampling and that mixing was limited to a thin layer (~3–4 cm; e.g. Muñoz et al., 2007) compared with the length of the core being analyzed (30 cm). Previous work at the same station indicates that the high flux of organic material during the upwelling season produced a dilution effect on the ^{210}Pb activities and, concomitantly, lower inventories in surface sediments; therefore we used the inventories in excess based on ash weight. At St. 18, the mixed layer varies seasonally between 2 and 5 cm (Muñoz et al., 2007); this did not affect significantly the annual inventories and allowed us to establish an accurate geochronology on a decadal scale.

3.2.3. Accumulation rates over the past ~150 years

Based on the age model, we calculated accumulation rates (AR) of Si_{OPAL} and siliceous microorganisms (Fig. 7) and combined these results with downcore changes in the relative abundance of diatom ecological groups (see below; Fig. 8) in order to provide a history of siliceous productivity in the area off Concepción for the recent past.

The Si_{OPAL} record showed a general trend of decreasing values from the base to the top of the core with three distinct drops at ~1855, 1940–1930 AD, and since the late 1990s (Fig. 7A). The most striking feature in the AR of diatoms was a decrease of almost one order of magnitude at 1910/1920 AD; before 1910 AD, AR averaged 1.6×10^6 valves cm^{-2} yr^{-1} and dropped to 2.9×10^5 valves cm^{-2}

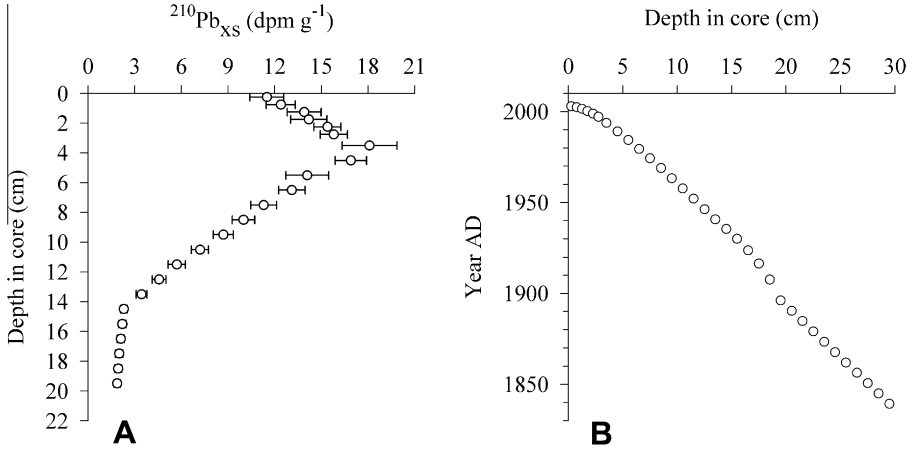

Fig. 6. (A) ^{210}Pb$_{xs}$ (in excess) distribution in sediment profile MUC1803. Horizontal lines indicate ±standard deviation. (B) Geochronology obtained from the total inventories of ^{210}Pb$_{xs}$; ages are expressed in AD years.

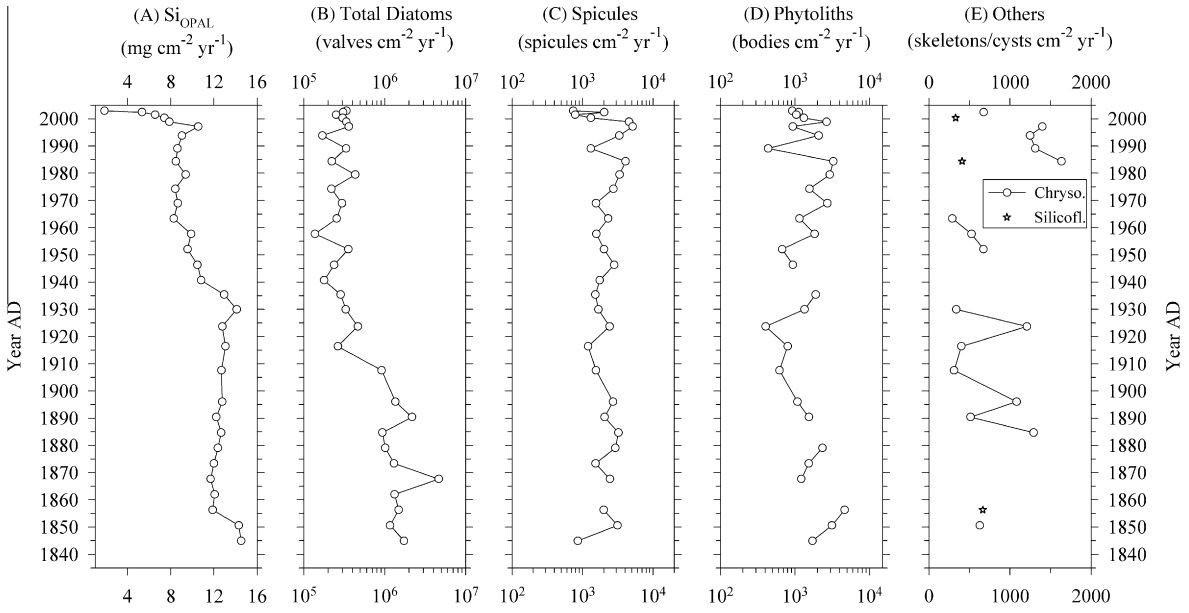

Fig. 7. Downcore accumulation rates of biogenic opal ((A) Si_{OPAL} in mg cm^{-2} yr^{-1}), and of the different groups of siliceous microorganisms (B–E) in core MUC1803 collected at Station 18, 1845–2003 AD. The age scale is in years AD.

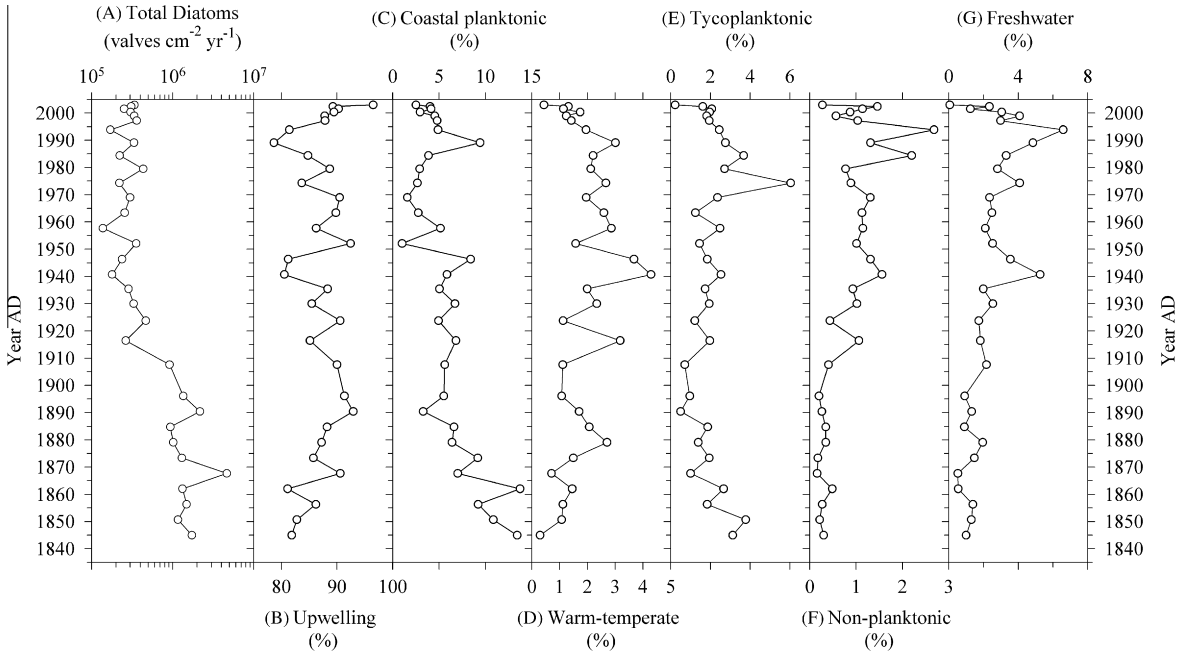

Fig. 8. Downcore accumulation rates of total diatoms (in valves cm^{-2} yr^{-1}) compared to the relative abundance of the six diatom ecological/distributional groups in core MUC1803 collected at Station 18 (see text for grouping of diatom species, and Table 2). The age scale is in years AD.

yr^{-1} thereafter (Fig. 7B). Accumulation rates of sponge spicules, on the other hand, were rather constant and fluctuated around 2×10^3 spicules cm^{-2} yr^{-1} (Fig. 7C). Phytoliths showed large fluctuations around a mean of $\sim 1.5 \times 10^3$ bodies cm^{-2} yr^{-1}, and were not found in several intervals of the older sediments; however, they were consistently present since ~1945 AD (Fig. 7D). Chrysophycean cysts showed very erratic behavior, and silicoflagellates were only present in three samples (2000, 1984, 1856 AD) (Fig. 7E).

All diatom species or groups of species were assigned to one of the following six ecological/distributional categories: upwelling, coastal planktonic (including species of temperate and cosmopolitan distribution), warm-temperate waters, tycoplanktonic, non-planktonic (including benthic, epiphytic, and/or epipelic habitats), and freshwater (Table 2). All along the core, sediments at St. 18 were characterized by the upwelling group (composed primarily of spores of several *Chaetoceros* species, *S. japonicum*, and *T. nitzschioides* var. *nitzschioides*; Table 2), which contributed, on average, >80% of the diatom assemblage. Despite the large drop in total diatom accumulation rates mentioned above, the upwelling assemblage as a whole did not change much (Fig. 8A and B), although a reduction in the relative abundance of *S. japonicum* (from >20% to 2%) was evident since the start of the 20th century. The coastal planktonic group (dominated by *Thalassiosira eccentrica* and *Coscinodiscus radiatus*) was second in importance, with an overall average

contribution of 6%. A decreasing trend characterized the older section of the core until the late 1800s; thereafter, values fluctuated around a mean of 4.5% (Fig. 8C). The overall contribution of the warm-temperate group (dominated by *Odontella longicruris*, spores of *Chaetoceros lorenzianus*, *Stephanopyxis palmeriana*, *Coscinodiscus janischii*) was 2%; it showed very low relative abundances (~1%) before 1875 AD and since the late 1990s, and was characterized by higher values (>2%) between those dates with distinct maxima at 1879, 1916, and 1940 to 1946 AD (Fig. 8D). The tycoplanktonic group was dominated by *Actinoptychus senarius*, with a general contribution of 2% and a maximum at 1974 AD (6%; Fig. 8E). The influence of the non-planktonic group, represented mainly by the genus *Cocconeis*, increased from the early 1900s until the mid-1990s (Fig. 8F). Finally, the general pattern of the freshwater diatom group (e.g. *Epithemia zebra*, *C. ventricosa*; Table 2) was similar to the non-planktonic group; their contribution increased around 1930 to 1940 AD and was highest (>4%) in 1940, 1974, and 1989 to 1993 AD (Fig. 8G).

4. Discussion

4.1. Water column patterns and the signal preserved in the surface sediments at Station 18

The coastal area off Chile between 35° and 38°S is recognized as one of the most productive areas in the world oceans. Here, strong seasonal coastal upwelling is the key process promoting the extremely high productivity (e.g. Daneri et al., 2000). Within this coastal upwelling ecosystem, the Time-Series Study of the COPAS Center off Concepción (~36°S), launched in 2002, has allowed an integrated view of the scales of variability (seasonal and inter-annual) in its physical, chemical and biological components (see Escribano and Schneider, 2007). Maxima in chlorophyll, nano- and microplankton, and zooplankton abundances are centered in the austral spring–summer period coincident with upwelling-favorable wind stress (e.g. Escribano et al., 2007; González et al., 2007; Montero et al., 2007; Sobarzo et al., 2007a). This pattern is repeated every year, although inter-annual variability in the strength and duration of the upwelling season has been observed (e.g. Escribano et al., 2007; Sobarzo et al., 2007a; Fig. 2A).

Our results on the temporal pattern of siliceous microorganisms (mainly diatoms) in the water column revealed that the highest monthly diatom abundances (>10^9 cells m^{-2} integrated over a water column depth of 40 m) always coincided with the upwelling period (Fig. 2B), and that the recurrent components of the spring–summer diatom assemblage were *S. japonicum* and several species of the genus *Chaetoceros* (Table 1). In the austral winter (non-upwelling season), on the other hand, intense precipitation and river discharges affect the salinity of the water column, and this freshwater flux inflicts the maximum annual stratification on the water column (Sobarzo et al., 2007a; Fig. 3). Suspended sediment loads increase from summer to winter in the Itata and Biobío rivers (Fig. 3A), and enrichment of lithogenic silica and microorganisms of continental origin below 50 m water depth (Sánchez et al., 2008) and in the surface sediments at St. 18 (Fig. 3D) may be invoked as the result of lateral advection and dispersal across the shelf from the increased river discharges into the shelf area in winter. In the upper water column, the diatom flora was more diverse than during the upwelling season (Fig. 2B), and *Pseudo-nitzschia* spp., *D. pumila* and *A. japonica* reached their highest relative abundances (Table 1); *Thalassiosira* blooms are sometimes observed in early autumn (González et al., 2007).

Given these two rather contrasting seasons in the area off Concepción, we evaluated whether the diatom flora deposited on the sea floor is representative of the seasonality of the original living assemblage in surface waters, and assessed the use of the information preserved in the sediments to interpret past productivity conditions. Based on our observations of the water column and surface sediments (Table 1; Fig. 2) in combination with those of González et al. (2007), we constructed schematic models that summarize the sedimentary imprint of the two contrasting seasons: the upwelling/high productivity of spring–summer and the non-upwelling/low productivity of autumn–winter. Because of the numerical dominance of diatoms in both the plankton and the sediments, these synoptic models focused mainly on this group (Fig. 9). The "spring–summer upwelling/productivity maximum/low diversity" of the surface waters (and high diatom sedimentation; González et al., 2007), with key diatom genera *Skeletonema* and *Chaetoceros*, was preserved in the sediments (showing attenuation of temporal variability) and represented by resting spores of several *Chaetoceros* species and valves of *S. japonicum* (Fig. 9A). Summer was a time of low river influence (Figs. 1C and 3A), with minor particle content of continental origin (e.g., freshwater diatoms, phytoliths, quartz, clays) (Fig. 9A).

On the other hand, significant plankton–sediment discrepancies were observed when comparing the assemblages of the "autumn–winter non-upwelling/low productivity/high diversity" period in the water column with those preserved in the surface sediments (Fig. 9B; Table 1). At that time, the enrichment of moderately resistant and robust taxa in the sediments (i.e. *Chaetoceros* spores, *A. senarius*, *O. longicruris*, and several freshwater diatoms) combined with the rarity or absence of delicate species (i.e. *Pseudo-nitzschia* spp., *D. pumila*, *A. japonica*, *C. closterium*) pointed to the preferential concentration in the sediments of certain species and the dissolution of others. The latter species are thin-walled, poorly silicified diatoms and do probably not withstand dissolution in the water column and/or at the seafloor. Therefore, a preservational bias was present in the sediments and a part of the original diversity (and probably also the total diatom abundance) was lost by dissolution processes. In addition, the enrichment of freshwater diatoms and phytoliths in winter surface sediments (~4%), which were negligible in the plankton, may be regarded as recorders of increased winter river discharges (Table 1; Figs. 3 and 9B).

Although we cannot provide information on each process that may have acted to modify the original living assemblage (e.g. zooplankton grazing, dissolution during settling, aggregation, lateral advection, bioturbation, resuspension; see review in Sancetta, 1989), the diatom assemblage in the surface sediments of St. 18 did contain several of the living species (Table 1). On an annual basis, vegetative cells of *Chaetoceros* and *Skeletonema* were found to dominate the water column (they are key groups in carbon fluxes on the Concepción shelf; González et al., 2007) whereas the surface sediment samples were dominated by resting spores of *Chaetoceros*, with the interlinking valves of *S. japonicum* being second in importance (Table 1). The very good preservation of delicate ornamental features of diatoms in our samples (Fig. 5) may be an indication of rapid export *via* flocculation and self-sedimentation, and deposition on the seafloor evading grazing or dissolution (see Grimm et al., 1996, 1997, and references therein). However, a factor that cannot be ruled out – especially for the dense, heavily silicified *Chaetoceros* spores – is the resuspension of previously deposited spores on the shelf and/or bottom current transportation to our sampling site. At St. 18, spores were continually present in the sediments at much higher levels than in the water column (Table 1). Although the sampling strategy used in the present study was not suitable to distinguish allochthonous introduction of spores, inertial motions over the continental shelf off Concepción are known to be important in shelf and shelf break areas, and to interact with bathymetry (submarine canyons, wide shelf, shelf break) and with upwelling events (Sobarzo et al., 2007b). Near-bottom

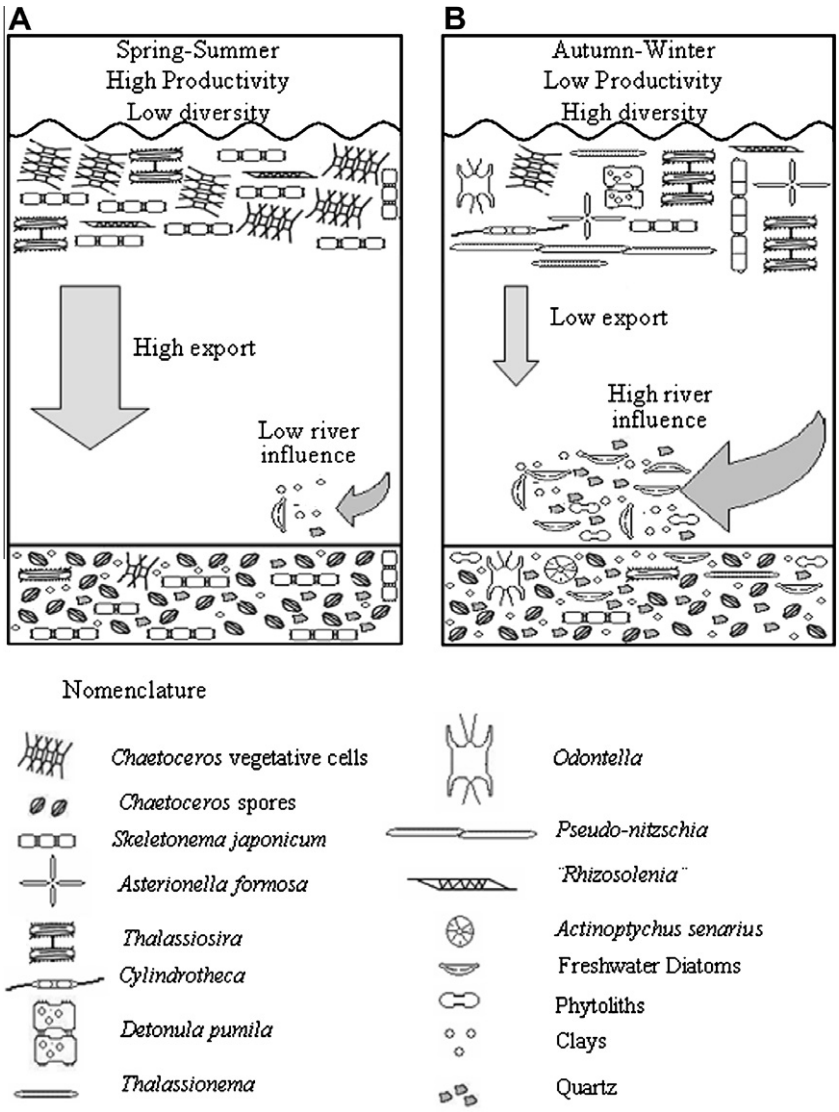

Fig. 9. Schematic models that summarize the sedimentary imprint of the two contrasting seasons in the area off Concepción, the upwelling/high productivity of spring–summer (A) and the non-upwelling/low productivity of autumn–winter (B), based on observations of the water column and surface sediments at Station 18 (see Table 1, and González et al., 2007).

currents measured close to St. 18 during late summer (upwelling conditions) by Sobarzo and Djurfeldt (2004) showed a mean southward sub-inertial flow of -4.0 cm s^{-1} with maximum southward values close to -10 cm s^{-1}. The intensification of bottom currents mainly occurs during downwelling periods and could play an important role in sediment resuspension over the shelf. Intensifications of near-inertial motions can induce near-bottom currents of 5–15 cm s^{-1} (Sobarzo et al., 2007b).

Diatom resting spore flux is characteristic of the spring bloom at temperate and high latitudes and is normally related to nitrogen depletion towards the end of the bloom (e.g. Hargraves and French, 1983; Garrison, 1984). The resting spore formation may ensure survival within coastal environments, and spores may seed the euphotic zone after the re-suspension of bottom sediments (e.g. Garrison, 1981; Pitcher, 1986; Sancetta and Calvert, 1988; McQuoid et al., 2002). In the area off Concepción, however, a recent study involving culture experiments of the flocculent layer deposited on surface sediments demonstrated that low dissolved oxygen availability in the bottom waters negatively affected the germination of *Skeletonema* and *Chaetoceros*, suggesting that they do not return to the water column (Sánchez et al., 2009). *Skeletonema* species are common diatoms in coastal estuarine and marine environments, where they often form dense blooms; *S. japonicum* in particular occurs in cool temperate coastal regions (see Kooistra et al., 2008, and references therein).

Sediment samples tend to yield a more integrated view than individual samples from live communities, and bioturbation by benthic fauna may lead to the homogenization of sediment assemblages, obscuring some of the original variability (Sancetta, 1989). Bioturbation at St. 18 affects mostly the upper 2–5 cm, and the depth of mixing varies seasonally and greatly depends on the faunal composition (weak vs. strong bioturbators; Muñoz et al., 2007). Although the end result may be an attenuation of the seasonal contrast (Sancetta, 1989), the temporal variability can still be identified in the surface sediments of St. 18. We summarized the seasonal contribution of upwelling, river runoff, diatoms and biogenic silica to the annual signal in the water column and in the surface sediments of St. 18 (Fig. 10), and found that although the direction of change was similar in both environments, the magnitude of the temporal variations in the sediments was either attenuated (for diatoms and runoff-continental signal), enhanced (diatom diversity), or bore no resemblance to the pattern in the

water column since the signal preserved could not be related to any combination of seasons (biogenic silica). Caution must thus be taken in the interpretation of biogenic opal from Concepción shelf surface sediments, since biogenic silica alone may tell us little about export productivity on these short-term scales and should be combined with detailed studies of microorganism assemblages (such as diatoms).

4.2. The sedimentary record of siliceous productivity over the past ~150 years

The sedimentary record from St. 18 off Concepción revealed a decrease of almost one order of magnitude in the diatom accumulation rates between the late 19th century and the beginning of the 20th century, specifically 1910–1920 AD (Fig. 8A). This drastic drop seemed to be accompanied by an increase in the magnetic susceptibility values and, roughly also, by an increase in the mean grain size of the total particles (Fig. 4). When looking into the diatom composition, the coastal upwelling and the warm-temperate groups (Fig. 8B and D) increased their contribution to the total assemblage during the second half of the 19th century (until ca. 1880–1890 AD) and had the highest variability in the 20th century (especially after ca. 1920 AD). This was accompanied by increasing contributions (and high variability) of freshwater diatoms during the 20th century (Fig. 8G). The patterns described suggest that the decrease in total diatoms since the late 19th/early 20th century could be related to an increase in the concentration of lithogenic particles due to enhanced continental runoff rather than a real reduction in siliceous phytoplankton productivity. The dilution of the sediments in the area off Concepción, with terrigenous material leading to low contents of metabolizable organic matter, has been previously reported by Bönning et al. (2005, 2009), who compared geochemical proxies of continental supply with marine organic carbon accumulation from sedimentary records at 36°S.

The general increase in decadal to interdecadal scale variability of the upwelling diatoms combined with the increased variability and higher concentrations of warm-temperate diatoms, alkenone concentrations and continental material from rivers (Fig. 4F and 8) seems to be coherent with an intensified influence of ENSO-like variability in the ocean-climate system off subtropical western South America since the late 19th century, as proposed previously for the coastal area off northern Chile at 23°S (Vargas et al., 2007). In fact, the greater influence of ENSO-like variability has resulted in increased frequency of rainfall since the late 19th century and during the 20th century through tropical–extratropical teleconnection mechanisms, as suggested by historical and instrumental records from central Chile, northern Peru and southern Ecuador (Ortlieb et al., 2002), leading to higher lithic components of fluvial origin in marine sediments (e.g., Rein, 2007) and implying regional hydrological changes (Vargas et al., 2006).The reconstruction of SST based on alkenones ($U^{K'}_{37}$ index, see methodology) from Concepción shelf sediments from 1840 to 2003 AD was compared to the instrumental SST record from the ICOADS database for roughly the same timeframe (Fig. 11). Despite the differences in spatial coverage (only two shelf stations vs. a grid of 3° in latitude), the large disparity in temporal resolution between instrumental and sedimentary records, and the inherent uncertainty associated with accurately dating sediment cores, the curves showed a general trend of increasing temperatures in the upwelling area off Concepción in the last ~70 years (Fig. 11). This is, of course, more evident in the ICOADS instrumental record. In this respect, the Concepción SST trends concurred with the conclusion that extensive global warming has occurred over the last century (e.g. see Gómez-Gesteira et al., 2008a for a review on coastal Atlantic sites; Field et al., 2006, and references therein for the California Current).

However, this general warming at 36°S contrasts with observations from northern Chile and southern Peru (Vargas et al., 2007), where decreased coastal SSTs since ~1878 AD were attributed to an intensification of upwelling-favorable coastal winds and increased primary export production during interdecadal El Niño-like periods of the 20th century. For recent decades, Falvey and Garreaud (2009) described a strong contrast between surface cooling at coastal stations and warming in the Andes, and proposed that the intensification of the South Pacific Anticyclone may play a role in maintaining cooler temperatures off the coast of Chile.

Bakun (1990) proposed that the major coastal upwelling systems of the world oceans have been experiencing increased upwelling intensity since the mid 20th century in response to anthropogenic greenhouse forcing through a mechanism of heating the land surface more than the ocean, thus enhancing the land-sea contrast that drives the upwelling process. This proposal was confirmed for several Eastern Boundary Current Systems (i.e., the Iberian Peninsula, the California Current, the northern part of the Peru–Chile Current) and the Arabian Sea (see Montecino and Lange, 2009, and references therein). However, in some cases, studies carried out in the same macro-region reached contradictory results. For example, in the Canary Upwelling System,

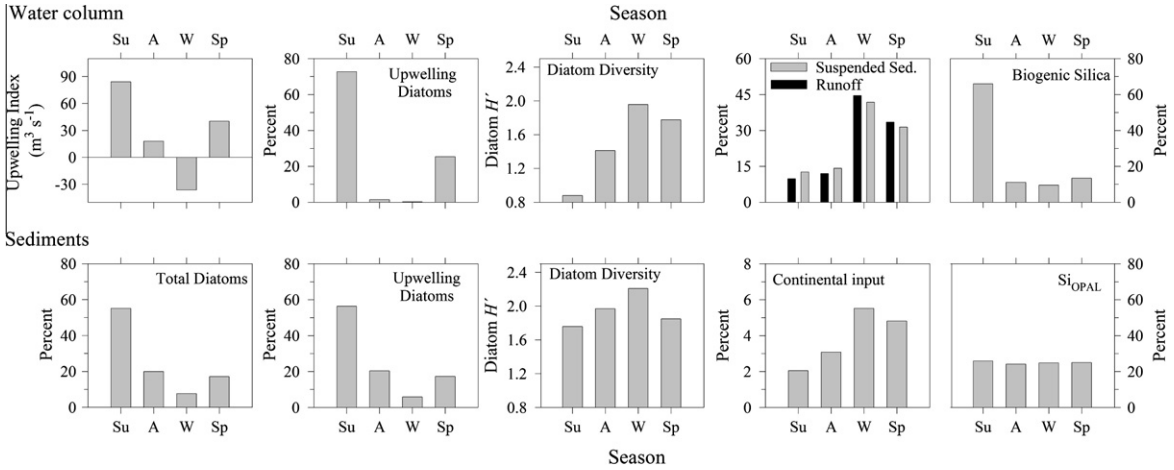

Fig. 10. Summary of the average seasonal contribution (%) to the annual signal (2002–2005) in the water column and in the surface sediments of Station 18 for: Upwelling Index, total diatoms, upwelling diatoms, diatom diversity, river runoff/continental signal and biogenic silica. Percent contribution refers to the seasonal average of each variable with respect to its annual, averaged over the period 2002–2005. Biogenic silica data for the water column (integrated over 30 m water depth) was taken from Sánchez et al. (2008) for April 2004 to May 2005. Biobío river data (runoff and suspended sediments), as in Fig. 3. A = autumn, W = winter, Sp = spring, Su = summer.

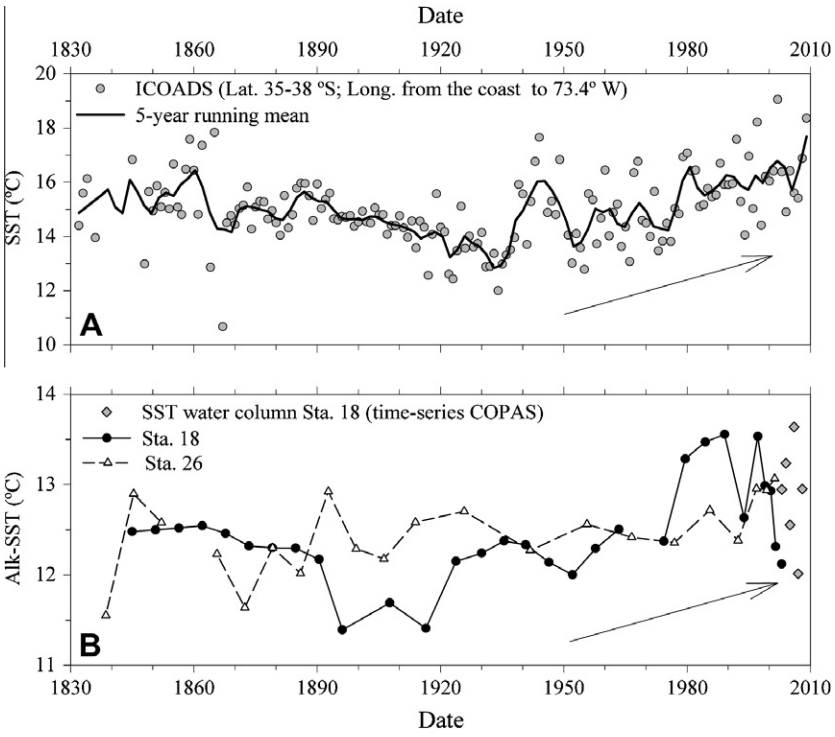

Fig. 11. (A) Sea surface temperature (SST) instrumental record from the International Comprehensive Ocean Atmosphere Data Set ICOADS (1832–2009) for the area 35–38°S and from the coast to 73.4°W. (B) Alkenone-derived SST records (1840–2003) from short shelf sediment cores collected off Concepción at Station 18 (36° 30.80′S; 73° 07.75′W; ~90 m water depth) and St. 26 (36° 25.67′S, 73° 23.34′W; 123 m water depth), and the annual average SST from COPAS time-series St. 18 (2003–2008). Note that the variability over the past ~20 years at St. 18 (black dots) matches the present-day range of SST variability from the COPAS time-series (grey diamonds). Alkenone-SST for St. 26 was taken from Vargas et al. (2007).

Gómez-Gesteira et al. (2008b) showed a strong decrease in upwelling intensity during all seasons over the past 40 years, contradicting the rapid 20th century increase reported by McGregor et al. (2007) off northwest Africa.

The observed temporal diatom patterns together with the SST warming trend in the Concepción area (especially from the ICOADS database), suggests a different mechanism operating here than the one proposed by Bakun (1990) and confirmed by Vargas et al. (2007) for northern Chile/southern Peru. The near-coastal increment in SST derived from our sedimentary record (St. 18) was not uniform. It showed a first ~0.7 °C increase in the 1920s, which was preceded by a period of cooling; the second warming (~1 °C) began in the late 1970s and seems to have lasted roughly 20 years at St. 18, whereas the ICOADS instrumental record showed continuous warming until present (Fig. 11). In addition, heightened variability over the past ~20 years and apparent cooling since 1999 AD can also be observed at nearshore St. 18.

Long-term SST records are scarce along the Chilean coast, and further research should include comparisons between shelf and oceanic high sedimentation sites in order to determine the real extent of 20th century warming in the Concepción area.

Acknowledgements

This research was funded by the Center for Oceanographic Research in the eastern South Pacific (COPAS) of the University of Concepcion (FONDAP Program Project No. 150100007). Project Fondecyt 11060484 (to GV) provided grain size and magnetic susceptibility data. Hydrographic data were derived from the COPAS Time-Series coastal St. 18 (http://copas.udec.cl/eng/research/serie/). The salinity profile in Fig. 3 was provided by R. Escribano. We thank the COPAS technical staff and the R/V Kay Kay crew for valuable help during the demanding field work. We are grateful to Alejandro Avila, Rodrigo Castro, Eduardo Menschel, Lilian Nuñez, and Valentina Flores for skilled laboratory work. The Stazione Zoologica "Anton Dohrn" in Naples, Italy, is acknowledged for the use of the electron microscope.

References

Ahumada, R., Chuecas, L., 1979. Algunas características hidrográficas de la Bahía Concepción (36 40′S-73 02′W) y áreas adyacentes, Chile. Gayana Miscelánea (Chile) 8, 1–56.

Alexander, A., Meunier, J.D., Lézime, A.M., Vicens, A., Schwartz, D., 1997. Phytoliths: indicators of grassland dynamics during the late Holocene in intertropical Africa. Palaeogeography, Palaeoclimatology, Palaeoecology 136, 213–229.

Appleby, P.G., Oldfield, F., 1978. The calculation of lead-210 dates assuming a constant rate of supply of unsupported ^{210}Pb to the sediment. Catena 5, 1–8.

Bakun, A., 1975. Daily and Weekly Upwelling Indices, West coast of North America 1967–1973. NOAA Technical Report NMFS SSRF-693.

Bakun, A., 1990. Global climate change and intensification of coastal upwelling. Science 247, 198–201.

Barnett, P.R., Watson, J., Connelly, D., 1984. A multiple corer for taking virtually undisturbed samples from shelf, bathyal and abyssal sediments. Oceanologica Acta 7, 399–408.

Berger, W., Smetacek, V., Wefer, G., 1989. Ocean productivity and paleoproductivity – an overview. In: Berger, W., Smetacek, V., Wefer, G. (Eds.), Productivity of the Ocean: Present and Past. John Wiley & Sons, pp. 1–34.

Bevington, P., Robinson, K., 1992. Error analysis. In: Bevington, P., Robinson, K. (Eds.), Data Reduction and Error analysis for the Physical Sciences. WCB/McGraw-Hill, USA, pp. 38–52.

Bloesch, J., Evans, R., 1982. Lead-210 dating of sediments compared with accumulation rates estimated by natural markers and measured with sediment traps. Hydrobiologia 92, 579–586.

Böning, P., Cuypers, S., Grunwald, M., Schnetger, B., Brumsack, H.J., 2005. Geochemical characteristics of Chilean upwelling sediments at 36 S. Marine Geology 220, 1–21.

Böning, P., Brumsack, H.J., Schnetger, B., Grunwald, M., 2009. Trace element signatures of Chilean upwelling sediments at 36 S. Marine Geology 259, 112–121.

Brower, J.E., Zar, J.H., Von Ende, C.N., 1998. Field and Laboratory Methods for General Ecology. McGraw-Hill, Dubuque, Iowa, USA, 194pp.

Chavez, F., Bertrand, A., Guevara-Carrasco, R., Soler, P., Csirke, J., 2008. The northern Humboldt Current System: brief history, present status and a view towards the future. Progress in Oceanography 79, 95–105.
Cochran, J.K., Frignani, M., Salamanca, M., Belluci, L.G., Guerzoni, S., 1998. Lead-210 as a tracer of atmospheric input of heavy metals in the northern Venice Lagoon. Marine Chemistry 62 (1–2), 15–29.
Cornejo, M., Farías, L., Gallegos, M., 2007. Seasonal cycle of N_2O vertical distribution and air-sea fluxes over the continental shelf waters off central Chile (36 S). Progress in Oceanography 75, 383–395.
Cupp, E., 1943. Marine plankton diatoms of the west coast of North America. Bulletin, Scripps Institution of Oceanography 5 (1), 1–238.
Daneri, G., Dellarossa, V., Quiñones, R., Jacob, B., Montero, P., Ulloa, O., 2000. Primary production and community respiration in the Humboldt Current system off Chile and associated oceanic areas. Marine Ecology Progress Series 197, 41–49.
Ellwood, B., 1980. Application of the anisotropy of magnetic susceptibility method as an indicator of bottom-water flow direction. Marine Chemistry 34, 783–790.
Escribano, R., Schneider, W. (Eds.), 2007. The structure and functioning of the coastal upwelling system off Central/Southern Chile. Progress in Oceanography, 75.
Escribano, R., Hidalgo, P., González, H.E., Giesecke, R., Riquelme-Bugueño, R., Manríquez, K., 2007. Seasonal and inter-annual variation of mesozooplankton in the coastal upwelling zone off central-southern Chile. Progress in Oceanography 75, 470–485.
Falvey, M., Garreaud, R.D., 2009. Regional cooling in a warming world: recent temperature trends in the southeast Pacific and along the west coast of subtropical South America (1979–2006). Journal of Geophysical Research 114, D04102.
Field, D.B., Baumgartner, T.R., Charles, C.D., Ferreira-Bartrina, V., Ohman, M.D., 2006. Planktonic foraminifera of the California Current reflect 20th-century warming. Science 311, 63–66.
Flynn, W., 1968. The determination of the low levels of Polonium-210 in environmental materials. Analytica Chimica Acta 43, 221–227.
Garrison, D.L., 1981. Monterey Bay phytoplankton. II. Resting spore cycle in coastal diatom populations. Journal of Plankton Research 3, 137–156.
Garrison, D.L., 1984. Planktonic diatoms. In: Steidinger, K.A., Walker, L.M. (Eds.), Marine Plankton Life Cycle Strategies. CRC Press, Boca Raton, pp. 1–17.
Gómez-Gesteira, M., De Castro, M., Álvarez, I., Gómez-Gesteira, J., 2008a. Coastal sea surface temperature warming trend along the continental part of the Atlantic Arc (1985–2005). Journal of Geophysical Research 113, C04010.
Gómez-Gesteira, M., De Castro, M., Álvarez, I., Lorenzo, M.N., Gesteira, J.L., Crespo, A.J., 2008b. Spatio-temporal upwelling trends along the Canary upwelling system (1967–2006). Trends and Directions in Climate Research: Annals of the New York Academy of Sciences 1146, 320–337.
González, H.E., Menschel, E., Aparicio, C., Barría, C., 2007. Spatial and temporal variability of microplankton and detritus, and their export to the shelf sediments in the upwelling area off Concepción, Chile (36 S), during 2002–2005. Progress in Oceanography 75, 435–451.
Graco, M., Farias, L., Molina, V., Gutiérrez, D., Nielsen, L., 2001. Massive development of microbial mats during phytoplankton bloom in an eutrophicated bay: implications on nitrogen cycling. Limnology and Oceanography 46, 821–832.
Grimm, K.A., Lange, C.B., Gill, A.S., 1996. Biological forcing of hemipelagic sedimentary laminae: evidence from ODP Site 893, Santa Barbara Basin, California. Journal of Sedimentary Research 66, 613–624.
Grimm, K.A., Lange, C.B., Gill, A.S., 1997. Self-sedimentation of fossil phytoplankton blooms in the geologic record. Sedimentary Geology 110, 151–161.
Grob, C., Quiñones, R., Figueroa, D., 2003. Cuantificación del transporte de agua costa-océano a través de filamentos y remolinos ricos en clorofila-a, en la zona centro-sur de Chile (35.5–37.5 S). Gayana 67 (1), 55–67.
Gutiérrez, D., Gallardo, V., Mayor, S., Neira, C., Vásquez, C., Sellanes, J., Rivas, M., Soto, A., Carrasco, F., Baltazar, M., 2000. Effects of dissolved oxygen and fresh organic matter on the bioturbation potential of macrofauna in sublittoral sediments off Central Chile during the 1997/1998 El Niño. Marine Ecology Progress Series 202, 81–99.
Hargraves, P.E., French, F.W., 1983. Diatom resting spores: significance and strategies. In: Fryxell, G.A. (Ed.), Survival Strategies of the Algae. Cambridge University Press, Cambridge, pp. 49–68.
Hormazábal, S., Núñez, S., Arcos, D., Espíndola, F., Yuras, G., 2004. Mesoscale eddies and pelagic fisheries off central Chile. Gayana 68 (1), 291–296.
Hustedt, F., 1930. Die Kieselalgen Deutschlands, Österreichs und der Scheiz. Dr. L. Rabenhorsts Kryptpgamen-flora von Deutschland, Österreichs und der Schweiz, 7(1), 920pp.
Kooistra, W., Sarno, D., Balzano, S., Gu, H., Andersen, R., Zingone, A., 2008. Global diversity and biogeography of *Skeletonema* species (Bacillariophyta). Protist 159, 177–193.
Letelier, J., Pizarro, O., Núñez, S., Arcos, D., 2004. Spatial temporal variability of the thermal fronts off central Chile (33–40 S). Gayana 2, 358–362.
McCaffrey, R., Thomson, J., 1980. Record of the accumulation of sediment and trace metals in the Connecticut salt marsh. Advances in Geophysics 22, 165–236.
McGregor, H.V., Dima, M., Fischer, H.W., Mulitza, S., 2007. Rapid 20th-century increase in coastal upwelling off northwest Africa. Science 315, 637–639.
McQuoid, R., Godhe, A., Nordberg, K., 2002. Viability of phytoplankton resting in the sediments of a coastal Swedish fjord. European Journal of Phycology 37, 191–201.
Montecino, V., Lange, C.B., 2009. The Humboldt Current System: ecosystem components and processes, fisheries, and sediment studies. Progress in Oceanography 83 (1–4), 65–79.
Montero, P., Daneri, G., Cuevas, L., González, H.E., Jacob, B., Lizárraga, L., Menschel, E., 2007. Productivity cycles in the coastal upwelling area off Concepción: the importance of diatoms and bacterioplankton in the organic carbon flux. Progress in Oceanography 75, 518–530.
Morales, C., González, H.E., Hormazábal, S., Yuras, G., Letelier, J., Castro, L., 2007. The distribution of chlorophyll-*a* and dominant planktonic components in the coastal transition zone off Concepción, central Chile, during different oceanographic conditions. Progress in Oceanography 75, 452–469.
Mortlock, R., Froelich, P., 1989. A simple method for the rapid determination of biogenic opal in pelagic marine sediments. Deep Sea Research Part A 36, 1415–1426.
Muñoz, P., Lange, C.B., Gutiérrez, D., Hebbeln, D., Salamanca, M., Dezileau, L., Reyss, J., Benninger, L., 2004. Recent sedimentation and mass accumulation rates based on ^{210}Pb along the Peru–Chile continental margin. Deep Sea Research Part II 51, 2523–2541.
Muñoz, P., Sellanes, J., Lange, C.B., Palma, M., Salamanca, M.A., 2007. Temporal variability of ^{210}Pb fluxes and bioturbation in shelf sediments beneath the high primary production area off Concepción, central-southern Chile (36 S). Progress in Oceanography 75, 586–602.
Ortlieb, L., Vargas, G., Hocquenghem, A.M., 2002. ENSO Reconstruction Based on Documentary Data from ECUADOR, Peru and Chile. PAGES (Past Global Changes)-News, 10(3), 14–17.
Pineda, V., 1999. El cañón submarino del Río Biobío: Aspectos dinámicos y ambientales. Ph.D. Thesis, Centro EULA, Universidad de Concepción, Chile (unpublished data).
Pitcher, G.C., 1986. Sedimentary flux and the formation of resting spores of selected *Chaetoceros* species at two sites in the southern Benguela System. South African Journal of Marine Science 4, 231–244.
Prahl, F.G., Wakeham, S.G., 1987. Calibration of unsaturation patterns in long-chain ketone compositions for paleotemperature assessment. Nature 330, 367–369.
Prahl, F.G., Muhlhausen, L.A., Zahnle, D.A., 1988. Further evaluation of long-chain alkenones as indicators of paleoceanographic conditions. Geochimica et Cosmochimica Acta 52, 2203–2310.
Rein, B., 2007. How do the 1982/83 and 1997/98 El Niños rank in a geological record from Peru? Quaternary International 161, 56–66.
Rivera, P., 1968. Sinopsis de las diatomeas de la Bahía de Concepción, Chile. Gayana Botánica 18, 1–112.
Rivera, P., 1981. Beiträge zur Taxonomie und verbreitung der gattung *Thalassiosira* Cleve. Bibliotheca Pycologica 56, 1–220.
Romero, O., Hebbeln, D., 2003. Biogenic silica and diatom thanatocoenosis in surface sediments below the Peru–Chile Current: controlling mechanisms and relationship with productivity of surface waters. Marine Micropaleontology 48, 71–90.
Round, F., Crawford, R., Mann, M., 1990. The Diatoms, Biology & Morphology of the Genera. Cambridge University Press, Cambridge, 747pp.
Runge, F., 1999. The opal phytolith inventory of soils in central Africa: quantities, shapes, classification, and spectra. Review of Palaeobotany and Palynology 107, 23–53.
Sancetta, C., 1989. Spatial and temporal trends of diatom flux in British Columbian fjords. Journal of Plankton Research 11 (3), 503–520.
Sancetta, C., Calvert, S.E., 1988. The annual cycle of sedimentation in Saanich Inlet, British Columbia: implications for the interpretation of diatom fossil assemblages. Deep Sea Research Part A 35 (1), 71–90.
Sánchez, G., Pantoja, S., Lange, C.B., González, H.E., Daneri, G., 2008. Seasonal changes in the biogenic and lithogenic silica off Concepción Bay (36 S) reflect marine productivity and continental input. Continental Shelf Research 28, 2594–2600.
Sánchez, G., Sarno, D., Montresor, M., Siano, R., Lange, C.B., 2009. Viabilidad de estados de resistencia de diatomeas y dinoflagelados en sedimentos marinos de dos áreas de surgencia de Chile. Gayana Botánica 66 (2), 239–255.
Schrader, H., Gersonde, R., 1978. Diatoms and silicoflagellates in the eight meters section of the lower Pliocene on Campo Rossello. Utrecht Micropaleontological Bulletin 17, 129–176.
Sims, P., [Ed.], 1996. An Atlas of British Diatoms. Biopress Ltd, UK. 601 pp.
Smol, J.P., 1988. Chrysophycean microfossils in paleolimnological studies. Palaeogeography, Palaeoclimatology, Palaeoecology 62, 287–297.
Sobarzo, M., Djurfeldt, L., 2004. Coastal upwelling process on a continental shelf limited by submarine canyons, Concepción, central Chile. Journal of Geophysical Research, 109(C12012), doi:10.1029/2004JC002350.
Sobarzo, M., Figueroa, D., Arcos, D., 1997. The Influence of winds and tides in the formation of circulation layers in a Bay, a case study: Concepción Bay, Chile. Estuarine, Coastal and Shelf Science 45, 729–736.
Sobarzo, M., Bravo, L., Donoso, D., Garcés-Vargas, J., Schneider, W., 2007a. Coastal upwelling and seasonal cycles that influence the water column over the continental shelf off central Chile. Progress in Oceanography 75, 363–383.
Sobarzo, M., Shearman, K., Lentz, S., 2007b. Near-inertial motions over the continental shelf off Concepción, central Chile. Progress in Oceanography 75, 348–362.
Strub, P., Mesías, J., Montecino, V., Rutllant, J., Salinas, S., 1998. Coastal ocean circulation off western South America. In: Robinson, A.R., Brink, K.H. (Eds.), The Sea, vol. 11. John Wiley & Sons, New York, pp. 273–314.

Takahashi, K., Blackwelder, P., 1992. The spatial distribution of silicoflagellates in the region of the Gulf Stream warm-core ring 82B: applications to water mass tracer studies. Deep Sea Research 39, 327–346.

Thiel, M., Macaya, E.C., Acuña, E., Arntz, W.E., Bastias, H., Brokordt, K., Camus, P.A., Castilla, J.C., Castro, L.R., Cortés, M., Dumont, C.P., Escribano, R., Fernández, M., Gajardo, J.A., Gaymer, C.F., Gomez, I., González, A.E., González, H.E., Haye, P.A., Illanes, J.E., Iriarte, J.L., Lancellotti, D.A., Luna-Jorquera, G., Luxoro, C., Manríquez, P.H., Marín, V., Muñoz, P., Navarrete, S.A., Perez, E., Poulin, E., Sellanes, J., Sepúlveda, H.H., Stotz, W., Tala, F., Thomas, A., Vargas, C.A., Vásquez, J.A., Alonso Vega, J.M., 2007. The Humboldt Current System of northern and central Chile-oceanographic processes, ecological interactions and socioeconomic feedback. Oceanogrraphy and Marine Biology Annual Review 45, 195–344.

Tomas, A. (Ed.), 1997. Identifying Marine Phytoplankton. Academic Press, San Diego, California, USA, 858pp.

Utermöhl, H., 1958. Zur Vervollkommnung der quantitativen Phytoplankton-Methodik. Mitteilungen Internationale Vereinigung für Theoretische und Angewandte Limnologie 1, 38.

Vargas, G., Rutllant, J., Ortlieb, L., 2006. ENSO tropical–extratropical climate teleconnections and mechanisms for Holocene debris flows along the hyperarid coast of western South America (17–24 S). Earth and Planetary Science Letters 249, 467–483.

Vargas, G., Pantoja, S., Rutllant, J., Lange, C.B., Ortlieb, L., 2007. Enhancement of coastal upwelling and interdecadal ENSO-like variability in the Peru–Chile Current since late 19th century. Geophysical Research Letters 34, L13607.

Witkowski, A., Lange-Bertalot, H., Metzeltin, D., 2000. Diatom flora of marine coast I. In: Lange-Bertalot, H., (Ed.), Iconographia Diatomologica. Annotated Diatom Micrographs, vol. 7. Diversity–Taxonomy-Identification. A.R.G. Gantner Verlag K.G., 925pp.